AMERICAN SOCIETY FOR MICROBIOLOGY | Applied and Environmental Microbiology®

ENVIRONMENTAL MICROBIOLOGY

Isoprenoid Quinones Resolve the Stratification of Redox Processes in a Biogeochemical Continuum from the Photic Zone to Deep Anoxic Sediments of the Black Sea

Kevin W. Becker,[a]* Felix J. Elling,[a]* Jan M. Schröder,[a] Julius S. Lipp,[a] Tobias Goldhammer,[b]* Matthias Zabel,[b] Marcus Elvert,[a] Jörg Overmann,[c] Kai-Uwe Hinrichs[a]

[a]Organic Geochemistry Group, MARUM–Center for Marine Environmental Sciences and Department of Geosciences, University of Bremen, Bremen, Germany

[b]Inorganic Geochemistry Group, MARUM–Center for Marine Environmental Sciences, University of Bremen, Bremen, Germany

[c]Leibniz Institute DSMZ–German Collection of Microorganisms and Cell Cultures, Braunschweig, Germany

ABSTRACT The stratified water column of the Black Sea serves as a model ecosystem for studying the interactions of microorganisms with major biogeochemical cycles. Here, we provide detailed analysis of isoprenoid quinones to study microbial redox processes in the ocean. In a continuum from the photic zone through the chemocline into deep anoxic sediments of the southern Black Sea, diagnostic quinones and inorganic geochemical parameters indicate niche segregation between redox processes and corresponding shifts in microbial community composition. Quinones specific for oxygenic photosynthesis and aerobic respiration dominate oxic waters, while quinones associated with thaumarchaeal ammonia oxidation and bacterial methanotrophy, respectively, dominate a narrow interval in suboxic waters. Quinone distributions indicate highest metabolic diversity within the anoxic zone, with anoxygenic photosynthesis being a major process in its photic layer. In the dark anoxic layer, quinone profiles indicate the occurrence of bacterial sulfur and nitrogen cycling, archaeal methanogenesis, and archaeal methanotrophy. Multiple novel ubiquinone isomers, possibly originating from unidentified intra-aerobic anaerobes, occur in this zone. The respiration modes found in the anoxic zone continue into shallow subsurface sediments, but quinone abundances rapidly decrease within the upper 50 cm below the sea floor, reflecting the transition to lower energy availability. In the deep subseafloor sediments, quinone distributions and geochemical profiles indicate archaeal methanogenesis/methanotrophy and potentially bacterial fermentative metabolisms. We observed that sedimentary quinone distributions track lithology, which supports prior hypotheses that deep biosphere community composition and metabolisms are determined by environmental conditions during sediment deposition.

IMPORTANCE Microorganisms play crucial roles in global biogeochemical cycles, yet we have only a fragmentary understanding of the diversity of microorganisms and their metabolisms, as the majority remains uncultured. Thus, culture-independent approaches are critical for determining microbial diversity and active metabolic processes. In order to resolve the stratification of microbial communities in the Black Sea, we comprehensively analyzed redox process-specific isoprenoid quinone biomarkers in a unique continuous record from the photic zone through the chemocline into anoxic subsurface sediments. We describe an unprecedented quinone diversity that allowed us to detect distinct biogeochemical processes, including oxygenic photosynthesis, archaeal ammonia oxidation, aerobic methanotrophy, and anoxygenic photosynthesis in defined geochemical zones.

KEYWORDS biomarkers, Black Sea, isoprenoid quinones, quinone profiles, sediments, stratified water column

Received 9 December 2017 **Accepted** 2 March 2018

Accepted manuscript posted online 9 March 2018

Citation Becker KW, Elling FJ, Schröder JM, Lipp JS, Goldhammer T, Zabel M, Elvert M, Overmann J, Hinrichs K-U. 2018. Isoprenoid quinones resolve the stratification of redox processes in a biogeochemical continuum from the photic zone to deep anoxic sediments of the Black Sea. Appl Environ Microbiol 84:e02736-17. https://doi.org/10.1128/AEM.02736-17.

Editor Volker Müller, Goethe University Frankfurt am Main

Address correspondence to Kevin W. Becker, kbecker@whoi.edu, or Felix J. Elling, felix_elling@fas.harvard.edu.

* Present address: Kevin W. Becker, Department of Marine Chemistry and Geochemistry, Woods Hole Oceanographic Institution, Woods Hole, Massachusetts, USA; Felix J. Elling, Department of Earth and Planetary Sciences, Harvard University, Cambridge, Massachusetts, USA; Tobias Goldhammer, Leibniz Institute of Freshwater Ecology and Inland Fisheries, Berlin, Germany.

K.W.B. and F.J.E. contributed equally to this work.

Microbially mediated redox reactions ultimately drive the global cycling of carbon, nitrogen, sulfur, and other active elements (1–3). On a cellular level, nonfermentative organisms utilize these redox reactions to maintain electron transport and proton gradients across the cytoplasmic membrane, which enables the generation of ATP and forms the basis of the cellular economy (4–6). Essential components of the electron transport chain are quinones, i.e., isoprenoid lipids that shuttle electrons and protons between membrane-bound protein complexes (5, 7). Isoprenoid quinones are commonly classified based on the structure of a polar cyclic headgroup and can be further distinguished by the length and degree of saturation of the head-to-tail-linked isoprenoid side chain (8, 9). The synthesis of structurally distinct quinones by eukaryotes and prokaryotes is determined both by phylogeny and, due to their distinct redox potentials (see Table S1 in the supplemental material), also by the specific requirements of the electron transport pathway (8, 10, 11).

The major classes of quinones in bacteria are polyunsaturated ubiquinones (UQs) and menaquinones (MKs), which operate in aerobic and anaerobic metabolisms, respectively. UQs are additionally involved in electron transport in the mitochondria and other organelles of eukaryotes (10). UQs typically contain six ($UQ_{6:6}$) to 10 ($UQ_{10:10}$), rarely up to 14, isoprenoid units, usually with one double bond per isoprenoid unit, here termed fully unsaturated (quinone nomenclature $Q_{m:n}$ indicates headgroup type Q, number of isoprenoid units in the side chain *m*, and number of double bonds *n*). Quinones that are specific for oxygenic photosynthetic eukaryotes and bacteria are vitamin K_1 (also known as phylloquinone or $MK_{4:1}$) and plastoquinones (predominantly $PQ_{9:9}$), which occur in photosystems I and II, respectively (10, 12, 13). In contrast to bacteria and eukaryotes, polyunsaturated quinones have been observed exclusively in only two archaeal lineages, the *Thermoplasmatales* and the *Halobacteriales* (14–16), the latter having acquired quinone biosynthesis genes from bacteria via lateral transfer (17). Most archaea produce saturated or partially unsaturated MKs with four to eight isoprenoid units (16), while specialized compounds are synthesized by some lineages, such as sulfur-containing quinones in *Sulfolobales* (16, 18, 19). The only organisms that have been suggested to not produce quinones are some fermentative bacteria and some representatives of the *Crenarchaeota* and *Euryarchaeota*, including methanogens (10, 16). However, methanogenic *Euryarchaeota* of the order *Methanosarcinales* are known to replace quinones with the functional analog methanophenazine (MP) (16, 20).

Given the large structural diversity (Fig. 1) and the detailed knowledge of their phylogenetic distribution, isoprenoid quinones offer a high potential as chemotaxonomic biomarkers (9, 16, 21–23). Besides the use of quinones to characterize microbial community structure, there is growing evidence that quinone abundance could be developed into a measure of metabolic activity. For example, chemostat experiments have demonstrated that the relative abundance of menaquinones increases with growth rates in the thaumarchaeon *Nitrosopumilus maritimus* (24). Further, quinones could be used as process biomarkers, as archaea and bacteria synthesize quinone types that reflect the biogeochemical conditions in their habitat (9, 16, 25) and remodel their quinone inventory when switching metabolic pathways on both the single-cell and community levels (11, 15, 23, 26, 27). Specifically, transitions from oxic to anoxic conditions and vice versa have been shown to induce rapid changes in quinone composition both in cultures (11, 15, 26) and incubation experiments with marine surface sediments (23). However, apart from thaumarchaeal quinones (16), quinone profiling has so far not been used to study microbial redox processes in the marine water column.

To demonstrate the utility of environmental quinone profiling, we studied a sequence of water column and sediment samples in the southern Black Sea (Fig. 2). Here, aerobic respiration depletes oxygen in the upper 60 to 120 m of the water column, while a shallow halocline leads to permanent water column stratification and thus prevents oxygenation of deeper waters (28). This oxic-anoxic interface is associated with a multilayered, temporally and spatially variable chemocline (29–31). Within the chemocline, microbes mediate a cascade of redox processes that can be traced by the

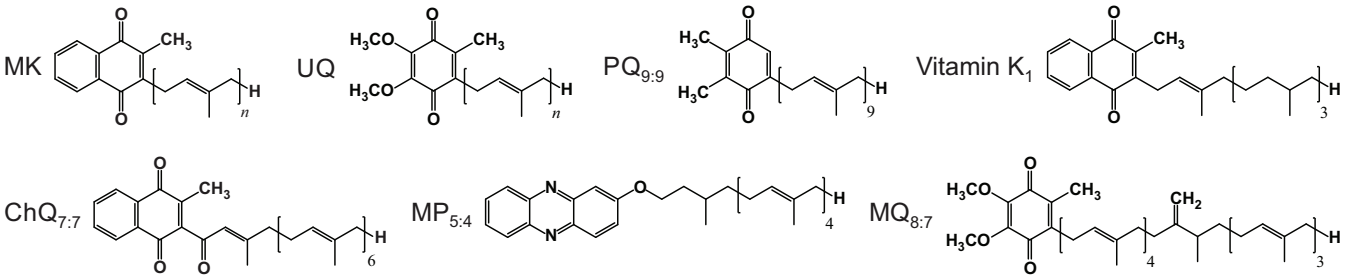

FIG 1 Structures of archaeal (MK and MP), bacterial (MK, UQ, PQ, ChQ, and MQ), and eukaryotal (UQ, PQ, and vitamin K_1) respiratory quinone classes detected in water column and sediment samples from the southern Black Sea. The length and degree of unsaturation of the isoprenoid side chains of quinones vary from 4 to 14 and from completely saturated to fully unsaturated, respectively, while known methanophenazines are exclusively comprised of five isoprenoid units. MK, menaquinone (vitamin K_2); UQ, ubiquinone; $MP_{5:4}$, methanophenazine; K_1, vitamin K_1 (synonyms, phylloquinone and $MK_{4:1}$); $ChQ_{7:7}$, chlorobiumquinone; $PQ_{9:9}$, plastoquinone; $MQ_{8:7}$, methylene-ubiquinone.

sequence of nitrogen, sulfur, and metal species (32, 33) and associated microbial biomarkers (34–37). Quantitatively important processes include ammonium and nitrite cycling by nitrifying archaea and bacteria as well as anaerobic ammonia-oxidizing bacteria (29, 38, 39), sulfide, and thiosulfate oxidation, e.g., by phototrophic green sulfur bacteria (40, 41) and *Shewanella* spp. (30, 42, 43), aerobic methane oxidation by *Alpha-* and *Gammaproteobacteria* (35), as well as bacterial Fe and Mn cycling (36, 44). In the anoxic zone, sulfate reduction and anaerobic oxidation of methane (AOM) are major microbial metabolisms (34, 35, 45, 46) that extend into the sediment (47).

While the depth distribution of the major sedimentary geochemical zones varies spatially, microbial processes form a continuum from the water column to the sediment of the Black Sea (47, 48). Sulfate reduction is the major carbon-remineralizing process in the surface sediments (49) due to the lack of other electron acceptors, such as nitrate, Fe^{3+}, and Mn^{4+} (50, 51). The sulfate reduction zone extends up to 4 m into the sediment and partially overlaps the underlying methanogenic zone (47, 49, 52). AOM occurs both within the surface sediment (46, 53) and within the comparatively broad sulfate methane transition zone (49).

Past studies of the Black Sea employed a variety of biomarker and activity assays to study either distinct processes (e.g., methanotrophy, nitrification, and anoxygenic photosynthesis) (29, 35, 40, 54) or subhabitats within the wider ecosystem (e.g., water column and surface sediment) (34, 36, 55). Here, we use isoprenoid quinone profiling, extending our earlier work on thaumarchaeal quinones in the Black Sea chemocline (16), to provide a detailed analysis of the stratification of microbial metabolisms in a continuum from the photic zone through the chemocline into the sedimentary deep biosphere.

RESULTS

Water column and sediment chemistry. Geochemical data revealed a strong vertical stratification of the Black Sea water column (Fig. 3). The salinity increased from 17.7 at the surface to 22.3 in deep waters. The steepest increase occurred in a discrete zone between 80 and 150 m below sea level (mbsl). Similarly, temperature increased with depth from 8.5 to 9°C. A fluorescence minimum was detected at 70 mbsl. Dissolved oxygen concentrations decreased in a narrow depth interval between 70 and 150 mbsl from >250 μmol kg^{-1} to below detection. Hydrogen sulfide (HS^-) was first detected at 100 m and slightly increased in concentration to 11.5 μmol $liter^{-1}$ at ca. 1,100 mbsl. Both dissolved phosphate (PO_4^{3-}) and ammonium (NH_4^+) were only detectable below 120 mbsl. PO_4^{3-} showed a distinct peak at 130 m followed by an increase from 300 mbsl into deeper waters, while NH_4^+ concentrations continuously increased toward the seafloor. Total Fe concentrations were relatively high in the uppermost water sample (0.31 μmol $liter^{-1}$ at 17 mbsl), decreased rapidly below this depth, showed a distinct peak at 111 mbsl (1.35 μmol $liter^{-1}$), and were generally high in the deeper waters. Although our analysis on water column samples could not

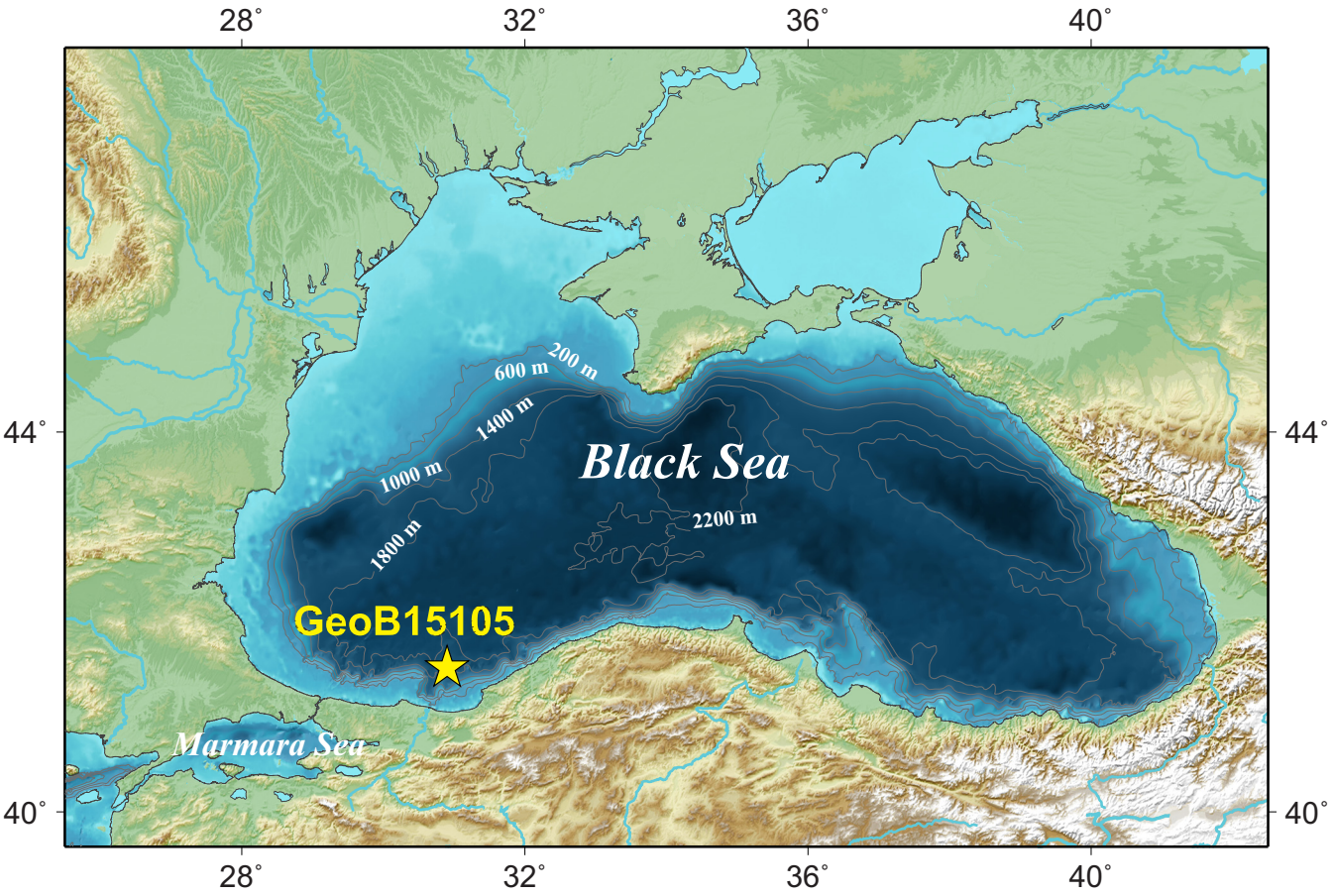

FIG 2 Location of the study site at the southern continental slope of the Black Sea (GeoB15105; 41°31.70′N, 30°53.10′E, 1,227-m water depth) sampled during R/V *Meteor* cruise M84/1. The map was generated using the GEBCO_08 bathymetric grid (version 2010092l; http://www.gebco.net) and Generic Mapping Tools version 5 (159).

distinguish between different valence states of iron, previous studies demonstrated that Fe^{3+} and Fe^{2+} are predominant in the oxic and anoxic zones, respectively (56, 57).

Based on the geochemistry, we defined the zonation of the water column at site GeoB15105 as an oxic zone from 0 to 70 mbsl, suboxic zone (chemocline; cooccurrence of HS^- and O_2) from 70 to 150 mbsl, and anoxic zone from 150 mbsl to the seafloor (~1,200 m).

The pore water profiles of dissolved PO_4^{3-} and NH_4^+ followed similar trends, with increasing concentrations within the first 250 cm below seafloor (cmbsf). Whereas NH_4^+ concentrations stayed fairly constant below 200 cmbsf, PO_4^{3-} slightly decreased toward the deepest investigated sample (815 cmbsf). Dissolved Fe^{2+} concentrations were below detection from 0 to 600 cmbsf and strongly increased from 600 to 800 cmbsf. Dissolved sulfate (SO_4^{2-}) concentrations decreased rapidly within the upper 90 cmbsf but remained above the detection limit down to 400 cmbsf. HS^- concentrations showed a maximum at approximately 100 cmbsf. Below 400 cmbsf, HS^- concentrations were close to zero. Methane concentrations were low (<75 μM) in the top 30 cm of the sediment but increased to almost 15.4 mM at 623 cmbsf. The $\delta^{13}C_{CH4}$ significantly decreased from −53‰ to −88.5‰ within the top 127 cmbsf. Below this depth, values increased to −69‰ at 815 cmbsf. Based on these results, the sulfate-methane transition zone (SMTZ) was assumed to cover the depth range from 80 to 400 cmbsf, with the core of the SMTZ at around 100 cmbsf.

Sediment lithology. The 8-m-long sediment core contains two major sedimentary units that have been recognized throughout the Black Sea basin (58–60). Unit I comprises laminated coccolith ooze (~1 to 3 wt% total organic carbon [TOC]) (Fig. 3E)

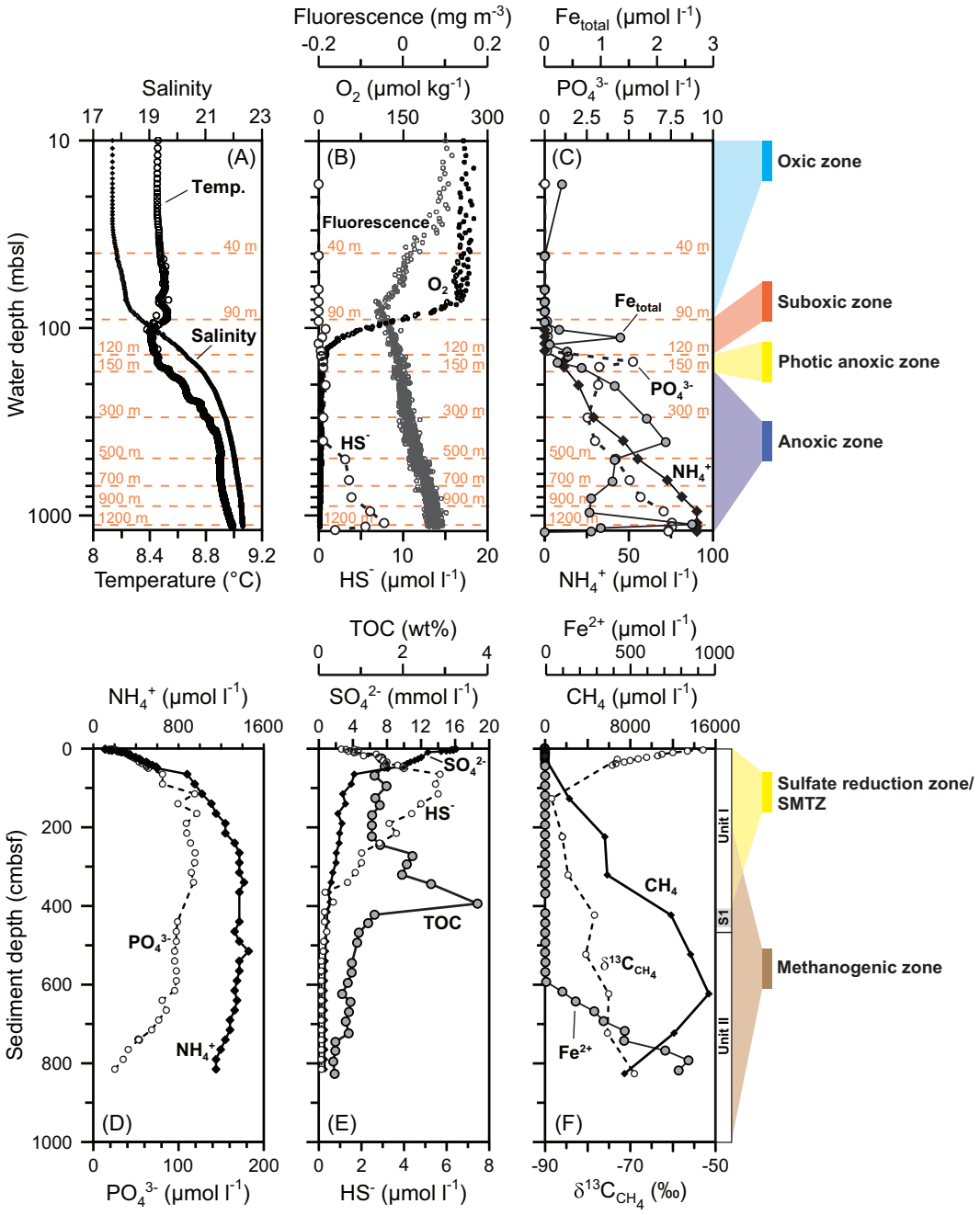

FIG 3 Black Sea water column and sediment pore water geochemistry. For the water column, salinity and temperature (A), chlorophyll *a* fluorescence, dissolved oxygen and hydrogen sulfide (B), and phosphate, total iron, and ammonium concentrations (C) are shown. Sampling depths for lipid and quinone analyses are indicated by orange dashed lines. Water depth is shown on a logarithmic scale (10 to 1,200 mbsl) in order to properly resolve the chemocline. For the sediments, pore water concentrations of phosphate and ammonium (D), total organic carbon (TOC), sulfate and hydrogen sulfide (E), and Fe^{2+}, methane, and $\delta^{13}C$ of methane (F) are shown.

deposited during the last 3 ka, while Unit II consists of organic-lean lacustrine deposits (Unit II, ~0.5 to 1 wt% TOC) overlain by an organic-rich sapropel (~4 wt% TOC) deposited from 7.5 to 3 ka before present (58, 59, 61), coeval to the development of water column anoxia in the Black Sea (60, 62).

Detection of conventional and novel quinones. Quinones detected in Black Sea suspended particulate matter and sediment samples comprised 43 different compounds, including vitamin K_1, $PQ_{9:9}$, chlorobiumquinone ($ChQ_{7:7}$), polyunsaturated UQs,

and MKs with variable chain lengths and degrees of unsaturation, fully saturated and monounsaturated MK_6, as well as the functional quinone analogs $MP_{5:3}$ and $MP_{5:4}$ (see Fig. S1 in the supplemental material). $ChQ_{7:7}$ was identified by accurate molecular mass and isotope pattern match of its proposed elemental formula in full scan mode, MS^2 fragment spectra (Fig. S2), and comparison of retention time and fragmentation pattern with $ChQ_{7:7}$ in extracts of an enrichment culture of the green sulfur bacterium *Chlorobium phaeobacteroides* BS1. We tentatively identified several novel UQ and MK isomers based on accurate molecular mass in full scan (MS^1) mode and characteristic fragmentation in MS^2 mode (Fig. S1). These isomers do not represent variable double-bond positions, since they were only detected for fully unsaturated (i.e., one unsaturation per isoprene unit) quinones. The quinones $PQ_{9:9}$ and $UQ_{7:7}$ to $UQ_{10:10}$ each showed one early [$Q_{m:n}$(a)] and one late [$Q_{m:n}$(b)] eluting isomer with highly similar MS^2 fragmentation. Based on comparison with the retention time of the commercially available $UQ_{10:10}$ (all-*trans*) standard, the early eluting UQ isomers (a-series) in our samples represent *trans*-isomers. Thus, the late eluting isomers (b-series) potentially represent compounds with one or more double bonds in *cis*-configuration. Up to four MK isomers with highly similar MS^2 fragmentations were detected, labeled consecutively a to d [$MK_{m:n}$(a-d)] from early to late eluting. MK and methyl-MK *cis*- and *trans*-isomers have previously been detected in the bacterium *Mycobacterium phlei* (63) and the archaeon *Thermoplasma acidophilum* (15). Thus, it is possible that the different isomers represent *cis* and *trans* isomers. However, with the analytical methods used in this study, configurational isomerism cannot be resolved.

Distribution of quinones in the Black Sea water column. Total quinone concentrations in the water column ranged between 0.21 and 9.4 ng liter^{-1} (Fig. 4). The highest concentrations in the water column were measured at 40 mbsl within the oxic zone and at 300 mbsl within the anoxic part of the water column. From the oxic zone to the chemocline, quinone concentrations decreased 7-fold. The lowest concentrations occurred in the deepest water column sample at 1,200 mbsl.

Concentration profiles and relative abundances of individual quinones were strongly linked to the geochemical zonation of the Black Sea water column. The photic zone, represented by the 40-mbsl sample, was characterized by high relative abundances and concentration maxima of vitamin K_1, $PQ_{9:9}$(a), and UQs but low relative and absolute abundances of MKs (Fig. 4 and Fig. S3). The upper chemocline (90 and 120 mbsl) samples were dominated by saturated MKs ($MK_{6:0}$ and $MK_{6:1}$; 70% of total quinones) with minor contributions of UQs and methylene-ubiquinone ($MQ_{8:7}$; structural identification shown in Fig. S2). The lower contribution of $MK_{6:0}$ and $MK_{6:1}$ to total quinones compared to previously reported values by Elling et al. (16) results from the detection of $MQ_{8:7}$, which was not included in the earlier study. Polyunsaturated MKs first occurred in the photic anoxic zone (150 m), and $ChQ_{7:7}$ was only observed in this zone (Fig. 4 and Fig. S3). The deep (aphotic) anoxic zone was characterized by high relative abundances of polyunsaturated MKs (up to ~50%) and UQs and minor contributions of $MQ_{8:7}$ and PQs (Fig. 4). While relative abundances of quinones were relatively uniform in the deep anoxic zone, most individual compounds showed distinct concentration profiles with either shallow maxima at 300 mbsl (e.g., $UQ_{8:8}$, $UQ_{10:10}$, $MK_{6:6}$, and $MQ_{8:7}$), deep maxima at 700 to 900 mbsl [e.g., $UQ_{9:9}$ and $MK_{10:10}$(b)], or at both depths [e.g., $UQ_{9:9}$(a), $MK_{7:6}$, and MPs; Fig. S3]. MPs were absent from the oxic part of the water column and the chemocline but were detected in the anoxic part of the water column, except at 1,200 mbsl (Fig. S3). Most notably, UQ isomers were detected only in the anoxic zone, and the concentration profiles of different MK and UQ isomers were highly divergent (Fig. S4).

To further constrain the sources of quinones, we compared their depth profiles with selected apolar microbial lipid biomarkers, such as cholesterol, as a general eukaryotic biomarker, alkenones for haptophyte algae, and isorenieratene (structural identification using high-performance liquid chromatography-mass spectrometry [HPLC-MS] as shown in Fig. S2) for anaerobic photosynthetic bacteria. Alkenones and cholesterol

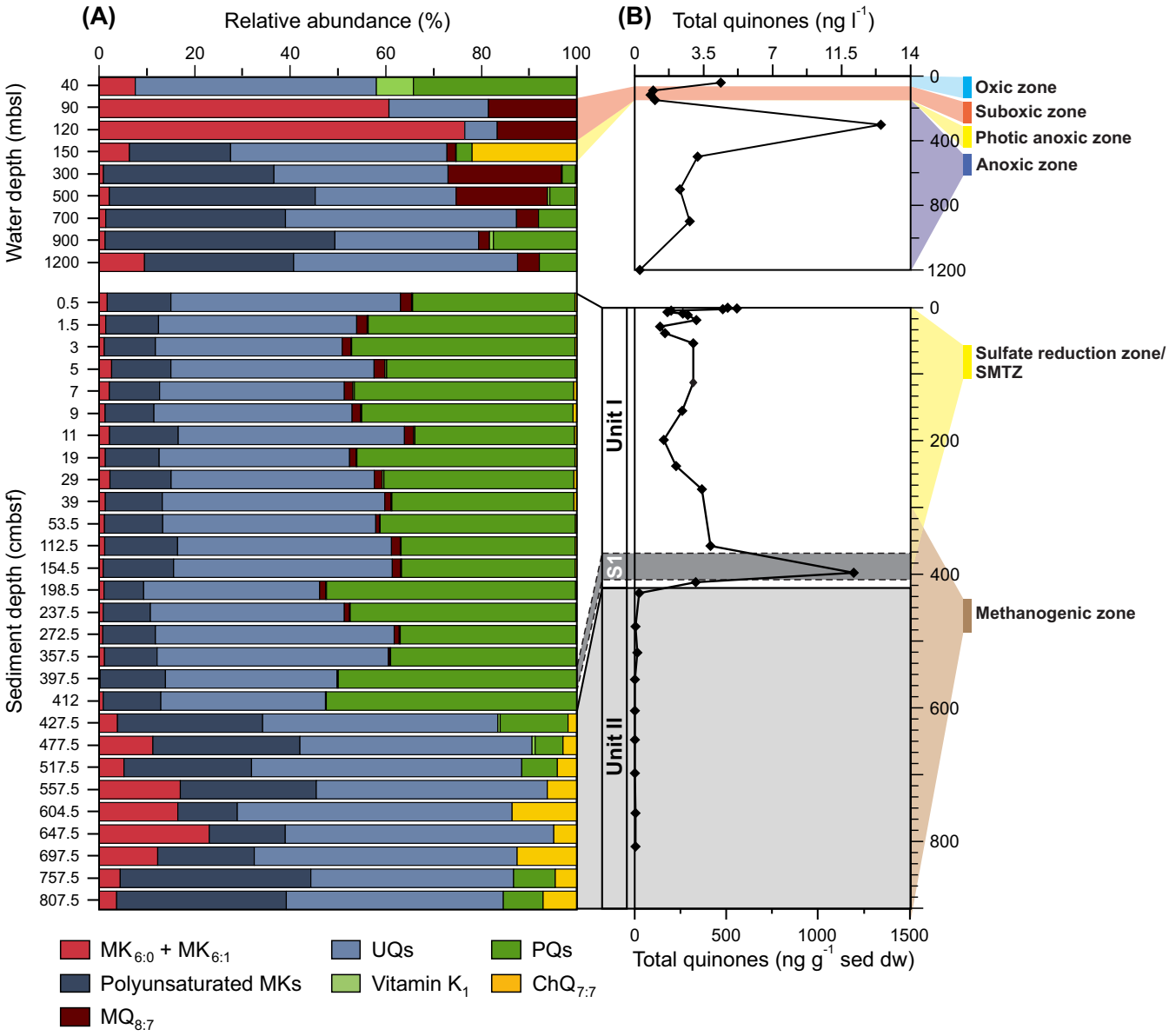

FIG 4 Relative (A) and absolute (B) abundances of major quinone classes in the water column and sediments of the southern Black Sea (cruise M84/1, station GeoB15105). Shaded area in the water column profile corresponds to the chemocline. In the sediment, the marine (Unit I; white) and lacustrine (Unit II; light gray) units, as well as the sapropel (S1; dark gray), are denoted. Quinone nomenclature is described in the legend to Fig. 1. Major geochemical zones are indicated on the right (SMTZ, sulfate-methane transition zone). MPs were analyzed under different conditions and therefore are not shown here (see Materials and Methods).

showed the highest abundances in the photic zone and followed the trend of vitamin K_1, $PQ_{9:9}$(a), and most UQs, while isorenieratene was only detected in the photic anoxic zone where $ChQ_{7:7}$ occurred (Fig. S3 and S5).

Distribution of quinones in the sediment. In the sediments, total quinone concentrations were highly variable and ranged from 2 to 1,000 ng g^{-1} sediment dry weight (sed. dw.) (Fig. 4). Highest concentrations were observed in the surface sediment and the sapropel layer (S1). Below the sapropel in lithological Unit II, concentrations were lowest and showed little variability.

Relative abundances of quinones differed between Unit I and Unit II sediments but were relatively uniform within each unit. Unit I sediments were dominated by UQs and PQs with minor amounts of polyunsaturated MKs, $MK_{6:0}$, $MK_{6:1}$, and $MQ_{8:7}$ (Fig. 4). Unit II sediments were characterized by higher relative abundances of UQs, $ChQ_{7:7}$, poly-

unsaturated MKs, $MK_{6:0}$, and $MK_{6:1}$ and lowered abundances of PQs. Absolute abundances of many quinones were dependent on the sedimentary unit, as were TOC and total quinones, showing a strong decrease in the upper 50 cmbsf, peaking at 398 cmbsf [e.g., vitamin K_1, $PQ_{9:9}$(a), $MK_{7:7}$(b)] or above [e.g., $MK_{7:7}$(a), $MK_{6:0}$, and $MK_{6:1}$], and low abundances in Unit II (Fig. S7). In contrast, concentrations of $MQ_{8:7}$, $ChQ_{7:7}$, and MPs gradually decreased with sediment depth irrespective of changes in lithological units. Multiple MK and UQ isomers were found only in the sediments and not in the water column [e.g., $MK_{7:7}$(a) and $UQ_{7:7}$(b)], and the relative abundances of isomers were different in the two sedimentary units and the water column. Additionally, concentration profiles of these isomers often diverged.

Like those of quinones, concentrations of apolar lipid biomarkers decreased strongly within the first 50 cmbsf (Fig. S5). In deeper sediments, concentrations varied distinctly, with alkenones showing no peak in the sapropel, cholesterol peaking only in the sapropel, and isorenieratene showing peaks at 113 cmbsf and in the sapropel at 398 cmbsf.

DISCUSSION

Potential of quinones for tracking biogeochemical stratification in the Black Sea water column. In the Black Sea water column, different quinones peaked at distinct, geochemically defined zones, indicating that quinones were produced *in situ* and rapidly turned over. This view agrees with earlier observations indicating high rates and efficiency of biomass turnover in the Black Sea, particularly in the oxic and suboxic zones (64). We used respiratory quinone profiling to examine the stratification of microbial communities and associated metabolic processes in the water column and the sediment. Metabolic stratification is indicated by the distinct clustering of quinone types, geochemical parameters, and sample depths in nonmetric multidimensional scaling (NMDS) analysis (see Fig. S8 in the supplemental material) as well as divergent quinone diversity indices (see the supplemental material). The biogeochemical zonation and the potential sources of quinones in the southern Black Sea are summarized in Table 1 and Fig. 5. Microbial communities and metabolisms in the water column were separated into (i) the oxic (photic) zone supporting oxygenic photosynthesis, (ii) the suboxic zone dominated by thaumarchaeal ammonia oxidation, (iii) the anoxic photic zone inhabited by sulfur-oxidizing photosynthetic bacteria, and (iv) the dark anoxic zone, which supports a variety of bacterial and archaeal metabolisms, such as methane oxidation, anaerobic ammonium oxidation (anammox), and sulfate reduction.

Oxic water column (0 to 90 mbsl): oxygenic photosynthesis and bacterial heterotrophy. The major quinone types in the oxic water column are associated with aerobic autotrophy and heterotrophy (UQs) as well as oxygenic photosynthesis [UQs, vitamin K_1, and $PQ_{9:9}$(a)] (9). Sources for $UQ_{9:9}$, $UQ_{10:10}$, vitamin K_1, and $PQ_{9:9}$(a) are both cyanobacteria and eukaryotic algae (8, 10, 12, 13), substantiated by their covariation with cholesterol and alkenones, while UQs with side chain lengths of 7 to 10 are additionally produced by alpha-, beta-, and gammaproteobacteria (9, 10). Only the *trans*-isomers (a-series) were detected in the oxic zone, indicating that aerobic organisms predominantly synthesize UQs with this specific stereochemical configuration.

The detection of $MK_{6:0}$ and $MK_{6:1}$ indicates the occurrence of *Thaumarchaeota* at 40 mbsl (16), although the concentrations of these quinones and the contribution to the overall quinone pool were comparatively low (Fig. 4). Accordingly, low thaumarchaeal biomass in the oxic zone was previously implicated by low concentrations of intact polar glycerol dibiphytanyl glycerol tetraethers observed previously (16), typical membrane lipids of planktonic *Thaumarchaeota* (83, 84).

Suboxic zone (90 and 120 mbsl): archaeal ammonia oxidation, bacterial sulfur, methane, and nitrite oxidation. The quinone composition in the suboxic zone of the water column is substantially different from that observed in the oxic zone. The depth profiles of the thaumarchaeal quinones $MK_{6:0}$ and $MK_{6:1}$ showed a distinct concentration maximum at 120 mbsl (Fig. 5 and Fig. S3), indicating maximum thaumarchaeal abundance in the chemocline, where both ammonia and oxygen are almost depleted

TABLE 1 Source organisms of quinones and associated biogeochemical processes in the stratified water column of the southern Black Sea

Zone and quinone type	(Putative) source organism	Biogeochemical process
Oxic (0–90 m)		
Vitamin K_1, $PQ_{9:9}$, $UQ_{7:7}$, $UQ_{9:9}$, $UQ_{10:10}$	Cyanobacteria, eukaryotic algae (9, 10)	Oxygenic photosynthesis
$UQ_{7:7}$, $UQ_{8:8}$, $UQ_{9:9}$, $UQ_{10:10}$	Diverse *Proteobacteria* (9, 10, 66)	Bacterial autotrophy and heterotrophy
Suboxic (90–120 m)		
$MK_{6:0}$, $MK_{6:1}$	*Thaumarchaeota* (16)	Ammonia oxidation
$UQ_{7:7}$, $UQ_{8:8}$, $UQ_{10:10}$	Alphaproteobacteria (9, 66) (e.g., *Nitrobacter* [68], type II methanotrophs [85])	Nitrite, iron, and aerobic methane oxidation
$UQ_{8:8}$	Betaproteobacteria (e.g., *Nitrosomonas* [69], *Thiobacillus* [70])	Ammonia, iron, and sulfur oxidation
$UQ_{8:8}$, $UQ_{9:9}$	Gammaproteobacteria (9, 66) (e.g., *Marinobacter* [71], *Thiomicrospira* [74], *Nitrosococcus*)	Ammonia, sulfur, iron, and nitrite oxidation
$MQ_{8:7}$, $UQ_{8:8}$	Gammaproteobacteria (9, 66) (e.g., type I methanotrophs [85])	Aerobic methane oxidation
Photic anoxic (120–150 m)		
ChQ, $MK_{7:7}$	Green sulfur bacteria (e.g., *Chlorobiaceae* [73])	Anoxygenic photosynthesis
Dark anoxic (150–1,200 m)		
$MK_{6:6}$	Deltaproteobacteria (9, 66) (e.g., *Desulfomonas* [75, 76], *Desulfovibrio* [75, 76])	Sulfate reduction
$MK_{6:6}$	*Epsilonproteobacteria* (9, 66, 79) (e.g., *Sulfurimonas*, *Sulfurovum* [92])	Sulfur oxidation
$MK_{6:6}$	*Planctomycetes* (9, 78, 80, 97)	Anaerobic ammonium oxidation
$MK_{7:7}$	Deltaproteobacteria (9, 66) (e.g., *Desulfobacter* [76], *Desulfococcus* [76], *Desulfosarcina* [76])	Sulfate reduction
$MK_{8:8}$	Deltaproteobacteria (9, 66) (e.g., *Desulfuromonas* [75])	Sulfate reduction
$MK_{7:7}$	*Firmicutes* (8) (e.g., *Desulfotomaculum* [75])	Sulfate reduction (e.g.)
$MK_{8:8}$, $MK_{8:7}$, $MK_{8:6}$, $MK_{9:9}$, $MK_{9:8}$, $MK_{9:7}$, $MK_{10:9}$, $MK_{10:10}$, $MK_{11:11}$	*Actinobacteria* (8, 9, 81, 160)	Nitrate reduction (e.g.)
$MP_{5:4}$, $MP_{5:3}$	*Methanosarcinales* (16, 20), potentially including ANME (117)	Methanogenesis, anaerobic oxidation of methane
Regular UQs	Unknown anaerobic source or fossil detritus	
UQ isomers	Unknown anaerobic source	
Vitamin K_1, $PQ_{9:9}$	Unknown anaerobic source or fossil detritus	

(16), which is in agreement with previous observations based on the abundances of thaumarchaeal 16S rRNA and ammonia-monooxygenase subunit A gene biomarkers (29, 38). The predominance of thaumarchaeal quinones (>70% of total quinones) (Fig. 4) and the decrease in dissolved ammonium concentration (Fig. 3) indicate that archaeal ammonia oxidation is the major respiratory process in this zone. Conversely, thaumarchaeal lipids have been found to comprise less than 10% of the combined bacterial and archaeal membrane lipids in this zone (16, 37), suggesting that microbial biomass in the chemocline is dominated by bacteria, whereas respiration is dominated by ammonia-oxidizing *Thaumarchaeota*. The high ratio of quinones relative to lipids (biomass) in *Thaumarchaeota* indicates high metabolic activity, as suggested by laboratory experiments (24), but may also reflect the low energy yield of ammonia oxidation that requires nitrifiers to oxidize 25 to 100 mol ammonia for each mole of CO_2 fixed (67).

The absence of quinones involved in photosynthesis indicates that photosynthetic cyanobacteria and eukaryotic algae either do not inhabit the suboxic zone or are metabolically not active. The UQs detected in the suboxic zone therefore likely originate from aerobic ammonia-, iron-, and sulfur-oxidizing alpha-, beta-, and gammaproteobacteria as well as aerobic nitrite- and methane-oxidizing alpha- and gammaproteobacteria (Table 1) (9, 85). The occurrence of these bacteria and biogeochemical processes in the Black Sea chemocline has also been attested by previous geochemical as well as gene and lipid biomarker surveys (34, 35, 86, 87). High relative abundances of a quinone specific for type I methanotrophs, $MQ_{8:7}$ (85), corroborate the importance

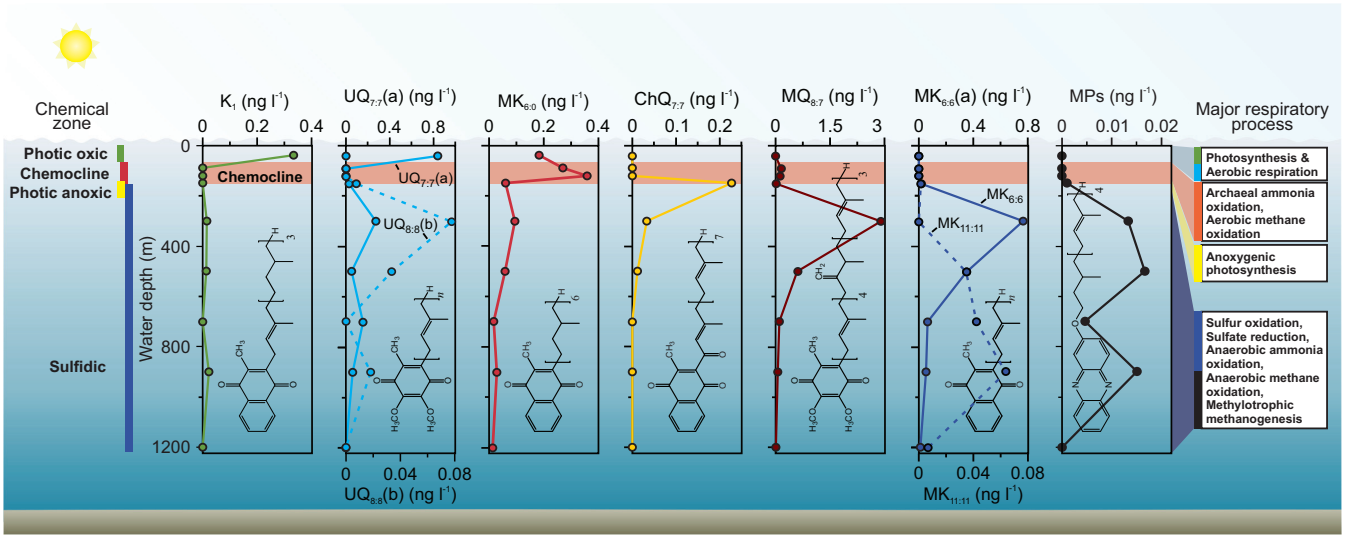

FIG 5 Depth profiles of selected quinones in the Black Sea water column. Red-shaded areas correspond to the chemocline. Note the different scales used on the *x* axes. Colors indicate different quinones associated with distinct microbial metabolisms: green, photosynthetic quinone vitamin K_1; light blue, bacterial ubiquinone [$UQ_{7:7}$(a), solid line; $UQ_{8:8}$(b), dashed line]; red, thaumarchaeal menaquinone ($MK_{6:0}$); dark blue, bacterial menaquinone [$MK_{6:6}$(a), solid line; $MK_{11:11}$, dashed line]; yellow, the green sulfur bacterial chlorobiumquinone ($ChQ_{7:7}$); dark red, the methane-oxidizing bacterial methylene-ubiquinone ($MQ_{8:7}$); black, *Methanosarcinales*-specific quinone analog methanophenazines (MPs).

of aerobic methanotrophy mediated by gammaproteobacteria in the Black Sea chemocline.

Photic anoxic zone (120 to 150 mbsl): bacterial anoxygenic photosynthesis. Penetration of H_2S-containing waters into the photic zone (Fig. 3) enables bacterial anoxygenic photosynthesis. Indeed, the carotenoid isorenieratene (88) and $ChQ_{7:7}$, which are both diagnostic for anaerobic phototrophic green sulfur bacteria of the family *Chlorobiaceae* (72, 89), showed distinct concentration maxima in anoxic, sulfidic waters at 150 mbsl (Fig. 5 and Fig. S3). This habitat depth is close to the maximum depth for anaerobic phototrophic growth calculated from the optical transparency of seawater (90). $MK_{7:7}$, which is a major quinone in the chlorosomes of *Chlorobiaceae* (72, 91), is the only MK that significantly increased in concentration at this depth (Fig. S3, b-isomer), suggesting a major contribution of these organisms to microbial activity in the deep chemocline. The abundance of a single *Chlorobium* species at depths of up to 145 mbsl has been reported to be a widespread feature of the Black Sea and attributed to extremely low-light adaptation of this particular phylotype (40, 41, 73). The peak of $ChQ_{7:7}$, the distinctive covariation with isorenieratene, as well as $MK_{7:7}$ indicate the high relative abundance of extremely low-light-adapted *Chlorobiaceae* in the Black Sea chemocline and validate the use of $ChQ_{7:7}$ as a biomarker for anoxygenic photosynthetic *Chlorobiaceae*.

Anoxic zone (150 to 1,200 mbsl): sulfate and nitrate reduction, anammox, and sulfur oxidation. Within the anoxic zone, quinone diversity indices are highest (Fig. S6) and abundances peak at concentrations more than 3-fold higher than those in the oxic and other layers (Fig. 4), indicating the highest microbial respiratory capacity. The first appearance of polyunsaturated MKs in the anoxic zone (including the photic, deep chemocline at 150 mbsl; Fig. 4 and Fig. S3) reflects a shift from aerobic and microaerobic archaeal and bacterial respiration to mainly bacterial, MK-dependent, anaerobic respiration. Likely sources of polyunsaturated MKs in the anoxic zone are diverse sulfate-reducing deltaproteobacteria, such as *Desulfobacter*, *Desulfococcus*, and *Desulfosarcina* spp., which produce predominantly $MK_{7:7}$ (76). Furthermore, *Desulfovibrio* and *Desulfuromonas* synthesize $MK_{6:6}$ and $MK_{8:8}$, respectively, as major quinones (8). Sulfur-oxidizing *Epsilonproteobacteria* previously detected in the Black Sea (36), e.g., *Sulfurimonas* and *Sulfurovum*, might represent additional sources of $MK_{6:6}$ (92). Potential sources for $MK_{7:7}$ and $MK_{9:9}$ are sulfate-reducing *Firmicutes* related to the genus

Desulfotomaculum (8). Several of these bacterial clades have been suggested to be responsible to a large extent for dark carbon fixation below the chemocline (93). The occurrence of quinones associated with sulfate-reducing bacteria in the anoxic zone is consistent with the abundance of bacterial ether lipids reported previously for this zone (37), which are almost exclusively associated with anaerobic bacteria (94) and particularly sulfate reducers (95, 96). An activity and abundance maximum of sulfate reducers and sulfur oxidizers in the upper anoxic zone is consistent with the observations that these bacteria first appear beneath the chemocline (34, 36, 77, 87) and that sulfur oxidation and sulfate reduction rates are highest in the upper anoxic zone of the Black Sea (30, 45).

Bacteria of the phylum *Planctomycetes* might represent an additional source of $MK_{6:6}$ (9, 78, 97). Bacteria affiliated with a deeply branching monophyletic lineage of this phylum perform the reduction of NO_2^- to N_2 by NH_4^+, i.e., anaerobic ammonium oxidation (anammox). Based on the analysis of 16S rRNA gene markers and the anammox-specific ladderane lipids, anammox bacteria have been shown to be present mainly within the suboxic zone of the Black Sea (34, 39). Moreover, previous studies proposed the cooccurrence and coupling of bacterial anammox and archaeal ammonia oxidation within the chemocline of the central Black Sea (29, 38). In contrast, the quinone profiles at our study site in the southern Black Sea suggest a vertical separation of the depth habitats of ammonia-oxidizing *Thaumarchaeota* and anammox bacteria by up to 200 m (Fig. 5), with *Thaumarchaeota* being confined to the suboxic zone and anammox bacteria residing within the upper anoxic zone (Table 1), although geochemical coupling of these processes cannot be excluded. High sulfide concentrations appear to inhibit growth of anammox bacteria (98), thus anammox bacteria are likely restricted to the upper part of the anoxic zone.

Actinobacteria are likely sources of fully unsaturated and partially saturated long-chain MKs, specifically of MK_8-MK_{11} (8, 99). Bacteria affiliated with this phylum have been implicated in denitrification, i.e., the heterotrophic reduction of NO_3^- to N_2, within the anoxic zone of the Black Sea (36). Quinones with 9 to 11 isoprenoid units are abundant in the anoxic zone of the Black Sea, especially in the deeper part (Fig. S3), suggesting a significant contribution of *Actinobacteria* to metabolic activity, possibly denitrification, in the deep anoxic Black Sea.

The occurrence of UQs, PQs, and $MQ_{8:7}$ in the anoxic zone is enigmatic, as these quinones are typically associated with aerobic metabolism. It is plausible that some anaerobic bacteria use ubiquinone-dependent pathways, as is the case for the nitrite-reducing methanotroph "*Candidatus* Methylomirabilis oxyfera" (100–102). Likewise, activity of methanotrophic bacteria (a source of UQs and $MQ_{8:7}$) that potentially use nitrate or nitrite instead of oxygen as the electron acceptor has been reported from the cores of marine oxygen minimum zones (103, 104). Methanotrophic bacteria could also be involved in cryptic Fe and methane cycling, as previously implied for other anoxic habitats (105–109). Alternatively, aerobic respiration might be supported by episodic lateral intrusions of modified Bosporus water that provide dissolved oxygen (as well as inorganic electron acceptors and fresh organic matter) to the suboxic and upper anoxic zones of the Black Sea (56, 110, 111). Although lateral intrusions and vertical transport could also deliver fossil quinones to the anoxic zone (e.g., see reference 64), the isomer pattern of UQs suggests *in situ* production of aerobic-type quinones: late eluting UQ isomers occurred only in the anoxic water column, while they were absent from the oxic and suboxic zones (Fig. S3 and S4).

Water column methane concentrations were not measured at our study site, but methane has been shown to be present at micromolar levels in the anoxic zone at other sites in the Black Sea (34, 46). While it was suggested that most of the methane in the Black Sea water column derives from the sediment (46), the detection of MPs (Fig. 5 and Fig. S3) indicates that methanogenesis also occurs within the anoxic waters. MPs are exclusively found in the archaeal order *Methanosarcinales* (16, 20), which comprises the metabolically most versatile methanogens utilizing $CO_2 + H_2$, acetate, and methylated compounds as substrates (112). Methanogens are likely outcompeted by sulfate-

reducing bacteria for acetate and H_2 due to thermodynamic constraints (113–115). Thus, utilization of noncompetitive methylated carbon substrates (114, 116) is a likely methanogenic pathway employed by *Methanosarcinales* in the Black Sea. However, anaerobic methanotrophic archaea (ANME-2), which are phylogenetically associated with the *Methanosarcinales*, have also been detected in the anoxic water column of the Black Sea (34, 35, 82). While the presence of MP in ANME-2 has not been confirmed, they have been implicated to function as electron carriers in these archaea (117), which may represent an additional source of MPs.

Other quinones specific for archaea, i.e., fully saturated menaquinones and naphthoquinones (16), were not detected in the anoxic zone of the Black Sea. This indicates that most anaerobic planktonic *Cren-* and *Euryarchaeota* either do not produce quinones or that these archaea synthesize bacterium-like polyunsaturated quinones similar to those found in extremely halophilic archaea of the order *Halobacteriales* (14) and thermophilic archaea of the order *Thermoplasmatales* (16), the latter being the closest cultivated relatives to the uncultivated planktonic marine group II *Euryarchaeota*, also found in the Black Sea (82, 118).

Lithological control on quinone distribution and fossilization of quinones in Black Sea sediments. Quinone concentrations are highest at the sediment surface and in the sapropel (Fig. S8A). The concentration maxima could be related to zones of higher activity, which would be consistent with higher microbial activity typically observed in shallow sediments (119) and organic matter-rich layers (120). On the other hand, these zones would show highest preservation (121, 122) if quinones derived from the water column would accumulate as molecular fossils. This dichotomy between the dependency of metabolic activity (and, thus, potentially quinone abundance) on organic matter availability and the possibly higher preservation of allochthonous quinones in high-TOC intervals poses significant challenges to the interpretation of sedimentary quinone profiles, because the fate of quinones after deposition, i.e., their degradation, transformation, and/or preservation, remains unknown. At least some quinones, such as PQs and vitamin K_1, likely are molecular fossils, as they are typically associated with aerobic metabolisms and/or phototrophy and their abundances are correlated with preserved oxic/photic zone lipid biomarkers, such as alkenones (haptophyte algae) and cholesterol (eukaryotes) (Fig. S5 and S10). However, normalization of quinone concentrations to TOC content (Fig. S9) reveals that quinone abundances are elevated in high-TOC intervals. Maxima in quinone concentrations thus may not be primarily controlled by preservation but could reflect higher standing stocks of metabolically active microbes. Further, the depth profiles of several quinones differ significantly from those of the putative fossil quinones (Fig. S7), and although preferential export and selective preservation could explain the observed signals, we hypothesize that most quinones were produced *in situ* by benthic microbes. We base this hypothesis on three lines of evidence. (i) Selective degradation of quinones is unlikely due to their highly similar chemical structures. (ii) We further observed distinct compositional changes between the water column and the sediments within different quinone classes, e.g., isomer distributions (Fig. S4). This becomes particularly apparent when the full diversity of quinones is considered (Fig. S11) and is supported by statistical analysis, which revealed distinct clusters of water column and sedimentary quinones in the NMDS space (Fig. S12). (iii) Some quinones, for example, $MK_{7:7}$(a), $MK_{7:7}$(d), $UQ_{11:11}$ (a), and $UQ_{11:11}$(b), were detected in the sediments but not in the water column. Together, these findings provide strong evidence that quinone compositions of planktonic and sedimentary communities differ.

The sedimentary quinone composition seems to be dependent on lithology. Relative abundance plots of major quinone groups (Fig. 4) and statistical analysis (NMDS) of individual quinone abundances revealed two clusters that align with lithological Unit I (euxinic marine) and Unit II (lacustrine) and correlate to some extent with the geochemical zonation (Fig. S12 and S13; see the next section for a more detailed discussion). We observed, for example, higher relative abundances of archaeal MKs, ChQ, and $MK_{8:8}$-$MK_{11:11}$ in Unit II than in Unit I as well as fine-scale compositional

changes within different quinone classes (Fig. S11). The quinone profiles thus agree with the hypothesis that community assembly and metabolisms in the deep sedimentary biosphere are determined by the initial community composition, and therefore the environmental conditions during sediment deposition (123–127), modulated by selective persistence (128). Within each lithological unit, the relative quinone compositions do not change with depth, not even in the sapropel. This invariance might be indicative of a high background signal of quinones associated with dormant or dead, but preserved, microbial biomass that likely masks *in situ* activity of a much smaller pool of living microorganisms. Still, the distributions of individual quinones allow the characterization of metabolic stratification, as discussed below.

Respiratory processes in Black Sea sediments. Three biogeochemical zones can be distinguished based on geochemical characteristics and quinone profiles: (i) the sulfate reduction zone, including the SMTZ; (ii) sapropel S1; and (iii) the methanogenic zone.

Concentrations of most quinones decrease within the first 50 cmbsf (Fig. 4 and Fig. S5), likely reflecting decreasing metabolic activity concomitant with gradual depletion of electron acceptors (e.g., sulfate) with depth (Fig. 3). Within the broad SMTZ (centered around ca. 80 to 150 cmbsf), concentrations of many quinones either stabilize or increase. Compounds that increase include several polyunsaturated MK isomers, e.g., $MK_{6:6}$(b), $MK_{7:7}$(d), and $MK_{8:8}$(c) (Fig. S7). Sulfate-reducing *Deltaproteobacteria*, possibly also engaged in AOM, are probable sources for these compounds. Similarly, MPs could originate from ANME archaea, which were previously detected in this depth interval (129) and which were suggested to utilize these quinone analogs (117). Saturated MKs, which are more prevalent than polyunsaturated MKs in cultivated archaea, were not abundant (apart from the thaumarchaeal $MK_{6:0}$ and $MK_{6:1}$), suggesting that benthic archaea do not produce them. Notably, some UQ isomers show peaks in concentration within the SMTZ (Fig. S7). The sources of and processes associated with these aerobic-type quinones in anoxic sediments remain unclear, but it is plausible that some anaerobic bacteria use ubiquinone-dependent pathways, as discussed above for the anoxic water column. A possible source of UQs could be methanotrophic bacteria involved in AOM coupled to iron reduction, as discussed above for the water column. Indeed, Fe^{2+} accumulates in the pore water of the methanogenic zone concomitant with a decrease in methane concentration (Fig. 3). This release of Fe^{2+} from the organic-poor, lacustrine sediment of Unit II is strikingly similar to lacustrine sediments of the Baltic Sea, where the occurrence of AOM coupled to iron reduction was suggested (105). The lack of MPs in this zone indicates that any archaea involved in this process are not *Methanosarcinales*. Quinones characteristic for type II methanotrophs (MQs) were not detected in this zone either, while $UQ_{8:8}$, the dominant quinone of type I aerobic methanotrophs (85), was a major component of the UQ pool (Fig. S11), potentially indicating activity of this clade.

Saturated and polyunsaturated MK concentrations peak either slightly above or within the sapropel (Fig. S7), indicating niche metabolic segregation. Coinciding concentration maxima of ammonia, phosphate (Fig. 3), and acetate (129) indicate enhanced heterotrophic activity in this zone. Due to a lack of electron acceptors, fermentation is likely to be the dominant heterotrophic process, as previously observed for deeply buried sapropels in the Mediterranean Sea (120). Multiple lineages of uncultivated archaea have been suggested to use heterotrophic and/or fermentative metabolisms (130–132), e.g., acetogenesis (133–135), and were reported to be abundant in the sediments studied here (*Bathyarchaeota*/MCG and MBG-D) (129). However, their quinone compositions remain unknown. Similarly, members of the candidate phylum "Atribacteria" (formerly OP9 and JS1), for which fermentation appears to be a characteristic metabolism (136, 137), were found in high relative abundances throughout the studied sediment core (129). While most fermenting bacteria do not produce isoprenoid quinones (8, 10), homoacetogens are a likely source for the high concentrations of MKs (e.g., $MK_{8:8}$) (138, 139) observed in the sapropel. Potential additional

sources of polyunsaturated MKs are *Chloroflexi*, i.e., green nonsulfur bacteria (9, 140), which were previously found to be abundant and metabolically active in Mediterranean sapropels (120) and other deep biosphere environments (128, 141). Collectively, geochemical and quinone biomarker evidence indicates that the sapropel supports high heterotrophic activity, which in turn may supply acetate and potentially other metabolites (e.g., H_2) to the sulfate reduction and methanogenic zones above and below the sapropel.

Based on methane concentrations and carbon isotope ratios as well as quinone distributions, methanogenesis likely occurs in two modes. The gradual decrease in MP concentration within the upper 400 cmbsf indicates that methanogenesis and methane oxidation by *Methanosarcinales* (including ANME-2) predominantly occurs within the sulfate reduction zone, where methanogenesis is likely methylotrophic. Further downcore, methane concentrations strongly increase to a maximum below the sapropel at ~630 cmbsf, indicating activity of methanogens other than *Methanosarcinales* and thus a vertical segregation of methylotrophic and hydrogenotrophic methanogens in Black Sea sediments. The methanogens inhabiting the deep sediments are likely obligate hydrogenotrophs such as *Methanobacteriales* or H_2-dependent methylotrophs such as *Methanomassiliicoccales*, which do not produce quinones or quinone analogs (16, 142, 143), or are affiliated with uncultured, potentially methanogenic lineages such as the *Bathyarchaeota* (144) or *Verstraetearchaeota* (65).

Conclusions. By using quinone profiling, a clear zonation of microbial diversity and redox processes could be resolved throughout the Black Sea water column and sediments. Coupled with geochemical data, quinone distributions indicated niche segregation between biogeochemical processes (e.g., photosynthesis, nitrification, aerobic methanotrophy, and anoxygenic photosynthesis) within the multilayered chemocline and anoxic zone (anammox, sulfate reduction, and methanogenesis/AOM) and continuation of anoxic aqueous community composition and respiration modes into shallow subsurface sediments. Within the sediment, segregation of microbial communities and respiration modes appeared to be driven by both lithology and geochemical gradients, with distinct quinone maxima around the sapropel reflecting intense heterotrophic activity.

Future work will need to target the relationship between biomass, metabolic activity (rates) and quinone abundances or distribution patterns, the source assignment of novel isomers, and the preservation potential of quinones in sediments. Cultivation experiments, polyphasic water column and sediment profiling studies, as well as development of methods for the isotopic analysis of quinones (e.g., for distinguishing MPs originating from methanogenic versus methane-oxidizing *Methanosarcinales*) will be needed to promote the utility of quinones as process biomarkers.

MATERIALS AND METHODS

Suspended particulate matter, sediment, and pore water sampling. Suspended particulate matter and sediment samples were collected in the southern Black Sea in February 2011 at site GeoB15105 (Fig. 2) during R/V *Meteor* cruise M84/1 (145). Suspended particulate matter was recovered at nine water depths, ranging between 40 and 1,200 m, by pumping 6 to 204 liters of seawater through two precombusted 0.7-μm-pore-size glass fiber filters in tandem using *in situ* pumps (see Table S2 in the supplemental material). Recovered filters were immediately wrapped in combusted aluminum foil and stored at −20°C. Due to the use of 0.7-μm-pore-size filters, membrane lipid and quinone concentrations should be regarded as minimum estimates (146). Water column profiles of temperature, chlorophyll *a* fluorescence, and depth, as well as pressure and dissolved oxygen, were measured with a vertical resolution of 1 m using a CTD rosette (GeoB15105-5). The salinity was derived from conductivity, while the density was calculated from pressure and temperature measurements as well as salinity. Water column samples (10 to 20 ml) were retrieved from these hydrocasts with Niskin bottles and directly filtered (0.2-μm syringe microfilter) after the recovery of the CTD rosette. Sediments were recovered using a multicorer (GeoB15105-4) and a gravity corer (GeoB15105-2). Sampling procedures were described in detail by Zabel et al. (145). In brief, samples for gas analyses were taken immediately after core recovery from the freshly cut surfaces after core extrusion (multicorer) or cutting into 1-m sections (gravity corer). The cores were then sealed with end caps and transferred to a cold room (4°C). In the cold room, pore water was extracted from sediment cores through holes in the core liner with Rhizon microsuction samplers (0.1-μm filter width; Rhizosphere Research Products, Wageningen, the Netherlands) immediately after core recovery and split into subsamples for offshore and onshore analysis (145).

After core splitting, sediment for lipid analyses was sampled in the cold room within 24 h after core recovery and stored at −20°C in brown glass bottles until solvent extraction.

Water column and pore water chemistry. Dissolved sulfate was determined by ion chromatography (Metrosep A Supp 5 column, with conductivity detection after chemical suppression; Metrohm Compact IC) in samples diluted 1:100 with Milli-Q-grade H_2O. Concentrations of dissolved phosphate were determined by forming phosphomolybdenum blue complexes (1 ml sample, 50 μl ammonium molybdate solution, 50 μl ascorbic acid solution, and 10 min of incubation) and measuring extinction at 820 nm using a Hach Lange DR 5000 spectrophotometer. Total dissolved iron (Fe_{tot}) was determined in HNO_3-acidified water samples by inductively coupled plasma optical emission spectroscopy (ICP-OES; axial plasma observation; Agilent 720). Ferrous iron (Fe^{2+}) was analyzed photometrically onboard directly after sample collection (147). Dissolved ammonium was detected with a flow injection, Teflon tape gas separator technique after Hall and Aller (148) using a temperature-compensated conductivity meter (no. 1056; Amber Scientific) equipped with a micro-flowthrough cell (529; Amber Scientific) and a strip chart recorder. Dissolved hydrogen sulfide was determined in samples fixed with $ZnCl_2$ using the photometric methylene blue method (149).

Hydrocarbon gases. Concentrations of dissolved methane were determined on board according to previously reported protocols (150, 151). In brief, 2 to 3 ml of wet sediment was incubated in a gas-tight 22-ml glass vial with a Teflon septum for 20 min at 60°C. After heating, 100- to 500-μl subsamples were taken from the headspace gas with a gas-tight syringe and analyzed by gas chromatography-flame ionization detection using a Carboxen-1006 PLOT fused-silica capillary column (0.32 mm by 30 m; Supelco, Inc., USA) on a ThermoFinnigan Trace GC. Methane concentrations were calculated from the partial pressure of methane in the headspace gas (calibrated against commercial standards; Scotty Laboratory Gases), headspace and sample volumes, and corresponding porosity data.

The stable carbon isotopic composition of methane was determined from duplicate analyses of the same samples using a Trace GC Ultra coupled to a Delta Plus XP isotope ratio mass spectrometer via a GC Combustion III interface (all ThermoFinnigan), as described previously (152). Carbon isotope ratios are reported in the δ-notation as per milliliter of deviation from the Vienna Pee Dee Belemnite (VPDB) standard. Analytical precision was determined by repeated injections of commercially available standards (methane at 100 ppm; Air Liquide) and was better than 1‰.

Total organic carbon. For TOC analysis, an aliquot (~3 g) of homogenized and freeze-dried sediment sample was decalcified by acidification with 10% HCl. After washing with water, centrifugation, and freeze drying, between 10 and 30 mg of decalcified sediment was weighed into tin capsules and analyzed in duplicate on a Thermo Scientific Flash 2000 elemental analyzer connected to a Thermo Delta V Plus IRMS (153). TOC concentrations refer to initial sediment dry weight (corrected for carbonate content determined by weighing before and after decalcification) and are reported in weight percent (wt%) with a limit of detection of 20 μg C.

Quinone and lipid extraction and analysis. Isoprenoid quinones and lipids were ultrasonically extracted from filters and sediments by following a modified Bligh & Dyer protocol (95) with dichloromethane-methanol-buffer (1:2:0.8, vol/vol/vol) using phosphate and trichloroacetic acid (CCl_3CO_2H) buffers (each 2×). The total lipid extract (TLE) was dried under a stream of N_2 and stored at −20°C until analysis.

TLEs were analyzed on a Dionex Ultimate 3000RS ultra-high-performance liquid chromatography (UHPLC) system connected to a Bruker maXis Plus ultra-high-resolution quadrupole time of flight tandem mass spectrometer (qToF-MS) equipped with an electrospray ionization (ESI) ion source operating in positive mode (Bruker Daltonik, Bremen, Germany). For quantification, a known amount of C_{46}-GTGT (glycerol trialkyl glycerol tetraether) standard was added to each sample before injection. Analytes were separated using reversed-phase (RP) HPLC on an ACE3 C_{18} column (2.1 by 150 mm; 3-μm particle size; Advanced Chromatography Technologies, Aberdeen, Scotland) maintained at 45°C as described previously (154).

The mass spectrometer was set to a resolving power of 27,000 at *m/z* 1,222, and every analysis was mass calibrated by loop injections of a calibration standard and correction by lock mass, leading to a mass accuracy of 1 to 3 ppm (155). Ion source and other MS parameters were optimized by infusion of standards into the eluent flow from the LC system using a T-piece. Quinones were identified by retention time, accurate molecular mass, and MS^2 fragmentation according to Elling et al. (16). Integration of peaks was performed on extracted ion chromatograms of ±10-mDa width and included the $[M+H]^+$, $[M+NH_4]^+$, and $[M+Na]^+$ ions. Where applicable, double-charged ions were included in the integration.

Additionally, selected samples were analyzed for low-abundance methanophenazines under the same chromatographic conditions on a Dionex Ultimate 3000RS UHPLC system connected to an ABSciEX QTRAP4500 triple-quadrupole/ion trap MS equipped with an ESI ion source operating in positive mode. Target compounds were detected by scheduled multiple-reaction monitoring of diagnostic tandem MS (MS/MS) transitions. Ion source, multiple-reaction monitoring transitions, and other MS parameters were optimized by direct infusion of commercially available standards as well as TLEs of *Nitrosopumilus maritimus* and *Methanosarcina acetivorans*.

Quinone abundances were corrected for the relative response of commercially available menaquinone ($MK_{4:4}$ for MKs, chlorobiumquinone [$ChQ_{7:7}$], and vitamin K_1) and ubiquinone ($UQ_{10:10}$, *trans*-isomer for UQs, and PQs) standards (Sigma-Aldrich, St. Louis, MO, USA) versus the C_{46}-GTGT standard. Due to a lack of an authentic standard, MP concentrations were not corrected for their relative response and thus are not included in total quinone abundance and distribution patterns or calculations of diversity indices. The abundances of isorenieratene were corrected by the relative response of a commercial β-carotene standard (Sigma-Aldrich). Similarly, the abundances of cholesterol and alkenones were corrected by the

relative response of a commercial cholesterol standard (Sigma-Aldrich) and synthetic $C_{37:2}$ and $C_{37:3}$ alkenone standards (156). The detection limits for quinones and lipids, as detected for authentic standards using the qToF and triple-quadrupole MS, were approximately 5 pg and 1 pg on column, respectively, depending on compound class and considering a signal-to-noise ratio of greater than 3.

Statistical analysis. Nonmetric multidimensional scaling (NMDS) analyses were performed in R (version 3.3.1 [157]) using the vegan package (version 2.4.2 [158]) separately on (i) water column suspended particulate matter, (ii) sediment quinone data sets, and (iii) the combined data sets. Normalized quinone concentrations (percent) were used for all statistical analyses, and geochemical/oceanographic parameters were fitted to the data. Geochemical/oceanographic parameters used for water column samples were temperature, fluorescence, salinity, O_2, NH_4^+, PO_4^{3-}, HS^-, and SO_4^{2-}. Geochemical parameters used for sediment samples were TOC, CH_4, $\delta^{13}C_{CH4}$, NH_4^+, PO_4^{3-}, HS^-, and SO_4^{2-}. For combined analyses, only parameters available for both sediments and water column (NH_4^+, PO_4^{3-}, HS^-, and SO_4^{2-}) were considered.

SUPPLEMENTAL MATERIAL

Supplemental material for this article may be found at https://doi.org/10.1128/AEM.02736-17.

SUPPLEMENTAL FILE 1, PDF file, 1.8 MB.

ACKNOWLEDGMENTS

We are grateful to the crew and the scientific shipboard party of R/V *Meteor*, cruise M84/1 (DARCSEAS I). L. Wörmer, V. B. Heuer, C. Zhu, T. B. Meador, and S. Pape are thanked for supporting sampling and instrumental analyses. We further thank N. I. Goldenstein for providing valuable feedback and supporting HPLC-MS analysis, F. Schmidt for support with statistical analyses, M. Könneke for providing constructive feedback to an earlier version of the manuscript, and I. D. Bull (University of Bristol) for providing alkenone standards. We thank two anonymous reviewers for helpful comments and suggestions.

This study was funded by the European Research Council under the European Union's Seventh Framework Programme–Ideas Specific Programme, ERC grant agreement no. 247153 (Advanced Grant DARCLIFE; principal investigator, K.-U.H.) and by the Deutsche Forschungsgemeinschaft through the Gottfried Wilhelm Leibniz Prize, awarded to K.-U.H. (Hi 616-14-1), and instrument grant Inst 144/300-1 (HPLC-qToF system).

REFERENCES

1. Dietrich LEP, Tice MM, Newman DK. 2006. The co-evolution of life and Earth. Curr Biol 16:395–400. https://doi.org/10.1016/j.cub.2006.05.017.
2. Falkowski PG, Fenchel T, Delong EF. 2008. The microbial engines that drive Earth's biogeochemical cycles. Science 320:1034–1039. https://doi.org/10.1126/science.1153213.
3. Newman DK, Banfield JF. 2002. Geomicrobiology: how molecular-scale interactions underpin biogeochemical systems. Science 296:1071–1077. https://doi.org/10.1126/science.1010716.
4. Mitchell P. 1961. Coupling of phosphorylation to electron and hydrogen transfer by a chemi-osmotic type of mechanism. Nature 191:144–148. https://doi.org/10.1038/191144a0.
5. Anraku Y. 1988. Bacterial electron transport chains. Annu Rev Biochem 57:101–132. https://doi.org/10.1146/annurev.bi.57.070188.000533.
6. Schäfer G, Engelhard M, Müller V. 1999. Bioenergetics of the Archaea. Microbiol Mol Biol Rev 63:570–620.
7. Gray HB, Ellis WR. 1994. Electron transfer, p 315–363. *In* Bertini I, Gray HB, Lippard SJ, Valentine JS (ed), Bioinorganic chemistry. University Science Books, Mill Valley, CA.
8. Collins MD, Jones D. 1981. Distribution of isoprenoid quinone structural types in bacteria and their taxonomic implications. Microbiol Rev 45:316–354.
9. Hiraishi A. 1999. Isoprenoid quinones as biomarkers of microbial populations in the environment. J Biosci Bioeng 88:449–460. https://doi.org/10.1016/S1389-1723(00)87658-6.
10. Nowicka B, Kruk J. 2010. Occurrence, biosynthesis and function of isoprenoid quinones. Biochim Biophys Acta 1797:1587–1605. https://doi.org/10.1016/j.bbabio.2010.06.007.
11. Bekker M, Kramer G, Hartog AF, Wagner MJ, de Koster CG, Hellingwerf KJ, de Mattos MJT. 2007. Changes in the redox state and composition of the quinone pool of *Escherichia coli* during aerobic batch-culture growth. Microbiology 153:1974–1980. https://doi.org/10.1099/mic.0.2007/006098-0.
12. Amesz J. 1973. The function of plastoquinone in photosynthetic electron transport. Biochim Biophys Acta 301:35–51. https://doi.org/10.1016/0304-4173(73)90011-6.
13. Brettel K, Leibl W. 2001. Electron transfer in photosystem I. Biochim Biophys Acta 1507:100–114. https://doi.org/10.1016/S0005-2728(01)00202-X.
14. Collins MD, Ross HNM, Tindall BJ, Grant WD. 1981. Distribution of isoprenoid quinones in halophilic bacteria. J Appl Bacteriol 50:559–565. https://doi.org/10.1111/j.1365-2672.1981.tb04258.x.
15. Shimada H, Shida Y, Nemoto N, Oshima T, Yamagishi A. 2001. Quinone profiles of *Thermoplasma acidophilum* HO-62. J Bacteriol 183:1462–1465. https://doi.org/10.1128/JB.183.4.1462-1465.2001.
16. Elling FJ, Becker KW, Könneke M, Schröder JM, Kellermann MY, Thomm M, Hinrichs K-U. 2016. Respiratory quinones in Archaea: phylogenetic distribution and application as biomarkers in the marine environment. Environ Microbiol 18:692–707. https://doi.org/10.1111/1462-2920.13086.
17. Nelson-Sathi S, Dagan T, Landan G, Janssen A, Steel M, McInerney JO, Deppenmeier U, Martin WF. 2012. Acquisition of 1,000 eubacterial genes physiologically transformed a methanogen at the origin of Haloarchaea. Proc Natl Acad Sci U S A 109:20537–20542. https://doi.org/10.1073/pnas.1209119109.
18. Thurl S, Witke W, Buhrow I, Schäfer W. 1986. Different types of quinones from sulphur-dependent archaebacteria. Biol Chem Hoppe Seyler 367:191–197. https://doi.org/10.1515/bchm3.1986.367.1.191.
19. De Rosa M, De Rosa S, Gambacorta A, Minale L, Thomson RH, Wor-

thington RD. 1977. Caldariellaquinone, a unique benzo[*b*]thiophen-4,7-quinone from *Caldariella acidophila*, an extremely thermophilic and acidophilic bacterium. J Chem Soc Perkin Trans 1 6:653–657. https://doi.org/10.1039/p19770000653.
20. Abken HJ, Tietze M, Brodersen J, Bäumer S, Beifuss U, Deppenmeier U. 1998. Isolation and characterization of methanophenazine and function of phenazines in membrane-bound electron transport of *Methanosarcina mazei* Gö1. J Bacteriol 180:2027–2032.
21. Urakawa H, Yoshida T, Nishimura M, Ohwada K. 2000. Characterization of depth-related population variation in microbial communities of a coastal marine sediment using 16S rDNA-based approaches and quinone profiling. Environ Microbiol 2:542–554. https://doi.org/10.1046/j.1462-2920.2000.00137.x.
22. Kunihiro T, Veuger B, Vasquez-Cardenas D, Pozzato L, Le Guitton M, Moriya K, Kuwae M, Omori K, Boschker HTS, van Oevelen D. 2014. Phospholipid-derived fatty acids and quinones as markers for bacterial biomass and community structure in marine sediments. PLoS One 9:e96219. https://doi.org/10.1371/journal.pone.0096219.
23. Hedrick DB, White DC. 1986. Microbial respiratory quinones in the environment. J Microbiol Methods 5:243–254. https://doi.org/10.1016/0167-7012(86)90049-7.
24. Hurley SJ, Elling FJ, Könneke M, Buchwald C, Wankel SD, Santoro AE, Lipp JS, Hinrichs K-U, Pearson A. 2016. Influence of ammonia oxidation rate on thaumarchaeal lipid composition and the TEX_{86} temperature proxy. Proc Natl Acad Sci U S A 113:7762–7767. https://doi.org/10.1073/pnas.1518534113.
25. Villanueva L, del Campo J, Guerrero R, Geyer R. 2010. Intact phospholipid and quinone biomarkers to assess microbial diversity and redox state in microbial mats. Microb Ecol 60:226–238. https://doi.org/10.1007/s00248-010-9645-2.
26. Nicolaus B, Trincone A, Lama L, Palmieri G, Gambacorta A. 1992. Quinone composition in *Sulfolobus solfataricus* grown under different conditions. Syst Appl Microbiol 15:18–20. https://doi.org/10.1016/S0723-2020(11)80131-1.
27. Sharma P, Teixeira de Mattos MJ, Hellingwerf KJ, Bekker M. 2012. On the function of the various quinone species in *Escherichia coli*. FEBS J 279:3364–3373. https://doi.org/10.1111/j.1742-4658.2012.08608.x.
28. Sorokin YI. 2002. The Black Sea: ecology and oceanography. Backhuys Publishers, Leiden, The Netherlands.
29. Coolen MJL, Abbas B, van Bleijswijk J, Hopmans EC, Kuypers MMM, Wakeham SG, Sinninghe Damsté JS. 2007. Putative ammonia-oxidizing Crenarchaeota in suboxic waters of the Black Sea: a basin-wide ecological study using 16S ribosomal and functional genes and membrane lipids. Environ Microbiol 9:1001–1016. https://doi.org/10.1111/j.1462-2920.2006.01227.x.
30. Jørgensen BB, Fossing H, Wirsen CO, Jannasch HW. 1991. Sulfide oxidation in the anoxic Black Sea chemocline. Deep Sea Res A Oceanogr Res Pap 38:S1083–S1103. https://doi.org/10.1016/S0198-0149(10)80025-1.
31. Murray JW, Jannasch HW, Honjo S, Anderson RF, Reeburgh WS, Top Z, Friederich GE, Codispoti LA, Izdar E. 1989. Unexpected changes in the oxic/anoxic interface in the Black Sea. Nature 338:411–413. https://doi.org/10.1038/338411a0.
32. Jannasch HW. 1991. Microbial processes in the black sea water column and top sediment: an overview, p 271–286. *In* İzdar E, Murray JW (ed), Black Sea oceanography. Springer, Dordrecht, The Netherlands.
33. Sorokin YI, Sorokin PY, Avdeev VA, Sorokin DY, Ilchenko SV. 1995. Biomass, production and activity of bacteria in the Black Sea, with special reference to chemosynthesis and the sulfur cycle. Hydrobiologia 308:61–76. https://doi.org/10.1007/BF00037788.
34. Wakeham SG, Amann R, Freeman KH, Hopmans EC, Jørgensen BB, Putnam IF, Schouten S, Sinninghe Damsté JS, Talbot HM, Woebken D. 2007. Microbial ecology of the stratified water column of the Black Sea as revealed by a comprehensive biomarker study. Org Geochem 38:2070–2097. https://doi.org/10.1016/j.orggeochem.2007.08.003.
35. Schubert CJ, Coolen MJL, Neretin LN, Schippers A, Abbas B, Durisch-Kaiser E, Wehrli B, Hopmans EC, Damsté JSS, Wakeham S, Kuypers MMM. 2006. Aerobic and anaerobic methanotrophs in the Black Sea water column. Environ Microbiol 8:1844–1856. https://doi.org/10.1111/j.1462-2920.2006.01079.x.
36. Fuchsman CA, Kirkpatrick JB, Brazelton WJ, Murray JW, Staley JT. 2011. Metabolic strategies of free-living and aggregate-associated bacterial communities inferred from biologic and chemical profiles in the Black Sea suboxic zone. FEMS Microbiol Ecol 78:586–603. https://doi.org/10.1111/j.1574-6941.2011.01189.x.
37. Schubotz F, Wakeham SG, Lipp JS, Fredricks HF, Hinrichs K-U. 2009. Detection of microbial biomass by intact polar membrane lipid analysis in the water column and surface sediments of the Black Sea. Environ Microbiol 11:2720–2734. https://doi.org/10.1111/j.1462-2920.2009.01999.x.
38. Lam P, Jensen MM, Lavik G, McGinnis DF, Müller B, Schubert CJ, Amann R, Thamdrup B, Kuypers MMM. 2007. Linking crenarchaeal and bacterial nitrification to anammox in the Black Sea. Proc Natl Acad Sci U S A 104:7104–7109. https://doi.org/10.1073/pnas.0611081104.
39. Kuypers MMM, Sliekers AO, Lavik G, Schmid M, Jørgensen BB, Kuenen JG, Sinninghe Damsté JS, Strous M, Jetten MSM. 2003. Anaerobic ammonium oxidation by anammox bacteria in the Black Sea. Nature 422:608–611. https://doi.org/10.1038/nature01472.
40. Marschall E, Jogler M, Henßge U, Overmann J. 2010. Large-scale distribution and activity patterns of an extremely low-light-adapted population of green sulfur bacteria in the Black Sea. Environ Microbiol 12:1348–1362. https://doi.org/10.1111/j.1462-2920.2010.02178.x.
41. Manske AK, Glaeser J, Kuypers MMM, Overmann J. 2005. Physiology and phylogeny of green sulfur bacteria forming a monospecific phototrophic assemblage at a depth of 100 meters in the Black Sea. Appl Environ Microbiol 71:8049–8060. https://doi.org/10.1128/AEM.71.12.8049-8060.2005.
42. Perry KA, Kostka JE, Luther GW, Nealson KH. 1993. Mediation of sulfur speciation by a Black Sea facultative anaerobe. Science 259:801–803. https://doi.org/10.1126/science.259.5096.801.
43. Jannasch HW, Wirsen CO, Molyneaux SJ. 1991. Chemoautotrophic sulfur-oxidizing bacteria from the Black Sea. Deep Sea Res A Oceanogr Res Pap 38:S1105–S1120. https://doi.org/10.1016/S0198-0149(10)80026-3.
44. Nealson KH, Myers CR, Wimpee BB. 1991. Isolation and identification of manganese-reducing bacteria and estimates of microbial Mn(IV)-reducing potential in the Black Sea. Deep Sea Res A Oceanogr Res Pap 38:S907–S920. https://doi.org/10.1016/S0198-0149(10)80016-0.
45. Albert DB, Taylor C, Martens CS. 1995. Sulfate reduction rates and low molecular weight fatty acid concentrations in the water column and surficial sediments of the Black Sea. Deep Sea Res I Oceanogr Res Pap 42:1239–1260. https://doi.org/10.1016/0967-0637(95)00042-5.
46. Reeburgh WS, Ward BB, Whalen SC, Sandbeck KA, Kilpatrickt KA, Kerkhof LJ. 1991. Black Sea methane geochemistry. Deep Sea Res A Oceanogr Res Pap 38:S1189–S1210. https://doi.org/10.1016/S0198-0149(10)80030-5.
47. Jørgensen BB, Böttcher ME, Lüschen H, Neretin LN, Volkov II. 2004. Anaerobic methane oxidation and a deep H_2S sink generate isotopically heavy sulfides in Black Sea sediments. Geochim Cosmochim Acta 68:2095–2118. https://doi.org/10.1016/j.gca.2003.07.017.
48. Knab NJ, Cragg BA, Hornibrook ERC, Holmkvist L, Pancost RD, Borowski C, Parkes RJ, Jorgensen BB. 2009. Regulation of anaerobic methane oxidation in sediments of the Black Sea. Biogeosciences 6:1505–1518. https://doi.org/10.5194/bg-6-1505-2009.
49. Jørgensen BB, Weber A, Zopfi J. 2001. Sulfate reduction and anaerobic methane oxidation in Black Sea sediments. Deep Sea Res Part 1 Oceanogr Res Pap 48:2097–2120. https://doi.org/10.1016/S0967-0637(01)00007-3.
50. Murray JW, Yakushev E. 2006. The suboxic transition zone in the Black Sea, p 105–138. *In* Neretin LN (ed), Past and present water column anoxia. Springer, Berlin, Germany.
51. Konovalov S, Samodurov A, Oguz T, Ivanov L. 2004. Parameterization of iron and manganese cycling in the Black Sea suboxic and anoxic environment. Deep Sea Res Part I Oceanogr Res Pap 51:2027–2045. https://doi.org/10.1016/j.dsr.2004.08.005.
52. Leloup J, Loy A, Knab NJ, Borowski C, Wagner M, Jørgensen BB. 2007. Diversity and abundance of sulfate-reducing microorganisms in the sulfate and methane zones of a marine sediment, Black Sea. Environ Microbiol 9:131–142. https://doi.org/10.1111/j.1462-2920.2006.01122.x.
53. Riedinger N, Brunner B, Lin Y-S, Voßmeyer A, Ferdelman TG, Jørgensen BB. 2010. Methane at the sediment-water transition in Black Sea sediments. Chem Geol 274:29–37. https://doi.org/10.1016/j.chemgeo.2010.03.010.
54. Egger M, Kraal P, Jilbert T, Sulu-Gambari F, Sapart CJ, Röckmann T, Slomp CP. 2016. Anaerobic oxidation of methane alters sediment records of sulfur, iron and phosphorus in the Black Sea. Biogeosciences 13:5333–5355. https://doi.org/10.5194/bg-13-5333-2016.

55. Thamdrup B, Rosselló-Mora R, Amann R. 2000. Microbial manganese and sulfate reduction in Black Sea shelf sediments. Appl Environ Microbiol 66:2888–2897. https://doi.org/10.1128/AEM.66.7.2888-2897.2000.
56. Lewis BL, Landing WM. 1991. The biogeochemistry of manganese and iron in the Black Sea. Deep Sea Res A Oceanogr Res Pap 38:S773–S803. https://doi.org/10.1016/S0198-0149(10)80009-3.
57. Landing W, Lewis B. 1991. Thermodynamic modeling of trace metal speciation in the Black Sea. Black Sea Oceanogr 351:125–160. https://doi.org/10.1007/978-94-011-2608-3_8.
58. Bahr A, Lamy F, Arz H, Kuhlmann H, Wefer G. 2005. Late glacial to Holocene climate and sedimentation history in the NW Black Sea. Mar Geol 214:309–322. https://doi.org/10.1016/j.margeo.2004.11.013.
59. Kwiecien O, Arz HW, Lamy F, Wulf S, Bahr A, Röhl U, Haug GH. 2008. Estimated reservoir ages of the Black Sea since the last glacial. Radiocarbon 50:99–118. https://doi.org/10.1017/S0033822200043393.
60. Eckert S, Brumsack HJ, Severmann S, Schnetger B, März C, Fröllje H. 2013. Establishment of euxinic conditions in the Holocene Black Sea. Geology 41:431–434. https://doi.org/10.1130/G33826.1.
61. Brumsack HJ. 1989. Geochemistry of recent TOC-rich sediment from the Gulf of California and the Black Sea. Geol Rundschau 78:851–882. https://doi.org/10.1007/BF01829327.
62. Arthur MA, Dean WE. 1998. Organic-matter production and preservation and evolution of anoxia in the Holocene Black Sea. Paleoceanography 13:395–411. https://doi.org/10.1029/98PA01161.
63. Dunphy PJ, Gutnick DL, Phillips PG, Brodie AF. 1968. A new natural naphthoquinone in *Mycobacterium phlei*. J Biol Chem 243:398–407.
64. Karl DM, Knauer GA. 1991. Microbial production and particle flux in the upper 350 m of the Black Sea. Deep Sea Res A Oceanogr Res Pap 38:S921–S942. https://doi.org/10.1016/S0198-0149(10)80017-2.
65. Vanwonterghem I, Evans PN, Parks DH, Jensen PD, Woodcroft BJ, Hugenholtz P, Tyson GW. 2016. Methylotrophic methanogenesis discovered in the archaeal phylum Verstraetearchaeota. Nat Microbiol 1:16170. https://doi.org/10.1038/nmicrobiol.2016.170.
66. Kersters K, De Vos P, Gillis M, Swings J, Vandamme P, Stackebrandt E. 2006. Introduction to the Proteobacteria, p 3–37. *In* Dworkin M, Falkow S, Rosenberg E, Schleifer K-H, Stackebrandt E (ed), The prokaryotes. Springer, New York, NY.
67. Ward BB. 2013. Nitrification. Reference module in earth systems and environmental science. Elsevier, San Diego, CA.
68. Aleem MIH, Sewell DL. 1984. Oxidoreductase systems in *Nitrobacter agilis*, p 185–210. *In* Strohl WR, Tuovinen OH (ed), Microbial chemoautotrophy. Ohio State University Press, Columbus, OH.
69. Hooper AB, Erickson RH, Terry KR. 1972. Electron transport systems of *Nitrosomonas*: isolation of a membrane-envelope fraction. J Bacteriol 110:430–438.
70. DiSpirito AA, Loh WHT, Tuovinen OH. 1983. A novel method for the isolation of bacterial quinones and its application to appraise the ubiquinone composition of *Thiobacillus ferrooxidans*. Arch Microbiol 135:77–80. https://doi.org/10.1007/BF00419487.
71. Spröer C, Lang E, Hobeck P, Burghardt J, Stackebrandt E, Tindall BJ. 1998. Transfer of *Pseudomonas nautica* to *Marinobacter hydrocarbonoclasticus*. Int J Syst Bacteriol 48:1445–1448. https://doi.org/10.1099/00207713-48-4-1445.
72. Frydman B, Rapoport H. 1963. Non-chlorophyllous pigments of *Chlorobium thiosulfatophilum* chlorobiumquinone. J Am Chem Soc 85:823–825.
73. Overmann J, Cypionka H, Pfennig N. 1992. An extremely low-light adapted phototrophic sulfur bacterium from the Black Sea. Limnol Oceanogr 37:150–155. https://doi.org/10.4319/lo.1992.37.1.0150.
74. Brinkhoff T, Muyzer G, Wirsen CO, Kuever J. 1999. *Thiomicrospira chilensis* sp. nov., a mesophilic obligately chemolithoautotrophic sulfur-oxidizing bacterium isolated from a *Thioploca* mat. Int J Syst Bacteriol 49:875–879. https://doi.org/10.1099/00207713-49-2-875.
75. Collins MD, Widdel F. 1986. Respiratory quinones of sulphate-reducing and sulphur-reducing bacteria: a systematic investigation. Syst Appl Microbiol 8:8–18. https://doi.org/10.1016/S0723-2020(86)80141-2.
76. Devereux R, Delaney M, Widdel F, Stahl DA. 1989. Natural relationships among sulfate-reducing eubacteria. J Bacteriol 171:6689–6695. https://doi.org/10.1128/jb.171.12.6689-6695.1989.
77. Lin X, Wakeham SG, Putnam IF, Astor YM, Scranton MI, Chistoserdov AY, Taylor GT. 2006. Comparison of vertical distributions of prokaryotic assemblages in the anoxic Cariaco Basin and Black Sea by use of fluorescence in situ hybridization. Appl Environ Microbiol 72:2679–2690. https://doi.org/10.1128/AEM.72.4.2679-2690.2006.
78. Sittig M, Schlesner H. 1993. Chemotaxonomic investigation of various prosthecate and/or budding bacteria. Syst Appl Microbiol 16:92–103. https://doi.org/10.1016/S0723-2020(11)80253-5.
79. Moss CW, Kai A, Lambert MA, Patton C. 1984. Isoprenoid quinone content and cellular fatty acid composition of *Campylobacter* species. J Clin Microbiol 19:772–776.
80. Kulichevskaya IS, Ivanova AA, Detkova EN, Rijpstra WIC, Sinninghe Damste JS, Dedysh SN. 2015. *Planctomicrobium piriforme* gen. nov., sp. nov., a stalked planctomycete from a littoral wetland of a boreal lake. Int J Syst Evol Microbiol 65:1659–1665. https://doi.org/10.1099/ijs.0.000154.
81. Collins MD, Pirouz T, Goodfellow M, Minnikin DE. 1977. Distribution of menaquinones in actinomycetes and corynebacteria. J Gen Microbiol 100:221–230. https://doi.org/10.1099/00221287-100-2-221.
82. Vetriani C, Tran HV, Kerkhof LJ. 2003. Fingerprinting microbial assemblages from the oxic/anoxic chemocline of the Black Sea. Appl Environ Microbiol 69:6481–6488. https://doi.org/10.1128/AEM.69.11.6481-6488.2003.
83. Pitcher A, Hopmans EC, Mosier AC, Park S-J, Rhee S-K, Francis CA, Schouten S, Sinninghe Damsté JS. 2011. Core and intact polar glycerol dibiphytanyl glycerol tetraether lipids of ammonia-oxidizing archaea enriched from marine and estuarine sediments. Appl Environ Microbiol 77:3468–3477. https://doi.org/10.1128/AEM.02758-10.
84. Elling FJ, Könneke M, Nicol GW, Stieglmeier M, Bayer B, Spieck E, de la Torre JR, Becker KW, Thomm M, Prosser JI, Herndl GJ, Schleper C, Hinrichs K-U. 2017. Chemotaxonomic characterisation of the thaumarchaeal lipidome. Environ Microbiol 19:2681–2700. https://doi.org/10.1111/1462-2920.13759.
85. Collins MD, Green PN. 1985. Isolation and characterization of a novel coenzyme Q from some methane-oxidizing bacteria. Biochem Biophys Res Commun 133:1125–1131. https://doi.org/10.1016/0006-291X(85)91253-7.
86. Konovalov S, Murray J, Luther G. 2005. Basic processes of Black Sea biogeochemistry. Oceanography 18:24–35. https://doi.org/10.5670/oceanog.2005.39.
87. Durisch-Kaiser E, Klauser L, Wehrli B, Schubert C. 2005. Evidence of intense archaeal and bacterial methanotrophic activity in the Black Sea water column. Appl Environ Microbiol 71:8099–8106. https://doi.org/10.1128/AEM.71.12.8099-8106.2005.
88. Repeta DJ, Simpson DJ. 1991. The distribution and recycling of chlorophyll, bacteriochlorophyll and carotenoids in the Black Sea. Deep Sea Res A Oceanogr Res Pap 38:S969–S984. https://doi.org/10.1016/S0198-0149(10)80019-6.
89. Overmann J. 2006. The family Chlorobiaceae, p 359–378. *In* Dworkin M, Falkow S, Rosenberg E, Schleifer K-H, Stackebrandt E (ed), The prokaryotes. Springer, New York, NY.
90. Repeta DJ. 1993. A high resolution historical record of Holocene anoxygenic primary production in the Black Sea. Geochim Cosmochim Acta 57:4337–4342. https://doi.org/10.1016/0016-7037(93)90334-S.
91. Frigaard NU, Takaichi S, Hirota M, Shimada K, Matsuura K. 1997. Quinones in chlorosomes of green sulfur bacteria and their role in the redox-dependent fluorescence studied in chlorosome-like bacteriochlorophyll c aggregates. Arch Microbiol 167:343–349. https://doi.org/10.1007/s002030050453.
92. Mino S, Kudo H, Takayuki A, Sawabe T, Takai K, Nakagawa S. 2014. *Sulfurovum aggregans* sp. nov., a novel hydrogen-oxidizing, thiosulfate-reducing chemolithoautotroph within the *Epsilonproteobacteria* isolated from a deep-sea hydrothermal vent chimney at the Central Indian Ridge, and an emended description of the genus *Sulfurovum*. Int J Syst Evol Microbiol 64:3195–3201. https://doi.org/10.1099/ijs.0.065094-0.
93. Pimenov NV, Neretin LN. 2006. Composition and activities of microbial communities involved in carbon, sulfur, nitrogen and manganese cycling in the oxic/anoxic interface of the Black Sea, p 501–521. *In* Neretin LN (ed), Past and present water column anoxia. Springer, Berlin, Germany.
94. Kim KC, Kamio Y, Takahashi H. 1970. Glyceryl ether phospholipid in anaerobic bacteria. J Gen Appl Microbiol 16:321–325. https://doi.org/10.2323/jgam.16.4_321.
95. Sturt HF, Summons RE, Smith K, Elvert M, Hinrichs K-U. 2004. Intact polar membrane lipids in prokaryotes and sediments deciphered by high-performance liquid chromatography/electrospray ionization multistage mass spectrometry–new biomarkers for biogeochemistry and

microbial ecology. Rapid Commun Mass Spectrom 18:617–628. https://doi.org/10.1002/rcm.1378.
96. Rütters H, Sass H, Cypionka H, Rullkötter J. 2001. Monoalkylether phospholipids in the sulfate-reducing bacteria *Desulfosarcina variabilis* and *Desulforhabdus amnigenus*. Arch Microbiol 176:435–442. https://doi.org/10.1007/s002030100343.
97. Ali M, Oshiki M, Awata T, Isobe K, Kimura Z, Yoshikawa H, Hira D, Kindaichi T, Satoh H, Fujii T, Okabe S. 2015. Physiological characterization of anaerobic ammonium oxidizing bacterium "*Candidatus* Jettenia caeni." Environ Microbiol 17:2172–2189.
98. Jensen MM, Kuypers MMM, Lavik G, Thamdrup B. 2008. Rates and regulation of anaerobic ammonium oxidation and denitrification in the Black Sea. Limnol Oceanogr 53:23–36. https://doi.org/10.4319/lo.2008.53.1.0023.
99. Urakawa H, Yoshida T, Nishimura M, Ohwada K. 2005. Characterization of depth-related changes and site-specific differences of microbial communities in marine sediments using quinone profiles. Fish Sci 71:174–182. https://doi.org/10.1111/j.1444-2906.2005.00945.x.
100. Ettwig KF, Butler MK, Le Paslier D, Pelletier E, Mangenot S, Kuypers MMM, Schreiber F, Dutilh BE, Zedelius J, de Beer D, Gloerich J, Wessels HJCT, van Alen T, Luesken F, Wu ML, van de Pas-Schoonen KT, Op den Camp HJM, Janssen-Megens EM, Francoijs K-J, Stunnenberg H, Weissenbach J, Jetten MSM, Strous M. 2010. Nitrite-driven anaerobic methane oxidation by oxygenic bacteria. Nature 464:543–548. https://doi.org/10.1038/nature08883.
101. Wu ML, De Vries S, Van Alen TA, Butler MK, Op Den Camp HJM, Keltjens JT, Jetten MSM, Strous M. 2011. Physiological role of the respiratory quinol oxidase in the anaerobic nitrite-reducing methanotroph "Candidatus Methylomirabilis oxyfera." Microbiology 157:890–898.
102. Padilla CC, Bristow L a, Sarode N, Garcia-Robledo E, Gómez Ramírez E, Benson CR, Bourbonnais A, Altabet MA, Girguis PR, Thamdrup B, Stewart FJ. 2016. NC10 bacteria in marine oxygen minimum zones. ISME J 10:2067–2071. https://doi.org/10.1038/ismej.2015.262.
103. Tavormina PL, Ussler W, Steele JA, Connon SA, Klotz MG, Orphan VJ. 2013. Abundance and distribution of diverse membrane-bound monooxygenase (Cu-MMO) genes within the Costa Rica oxygen minimum zone. Environ Microbiol Rep 5:414–423. https://doi.org/10.1111/1758-2229.12025.
104. Padilla CC, Bertagnolli A, Bristow LA, Sarode N, Glass J, Thamdrup B, Stewart F. 2017. Metagenomic binning recovers a transcriptionally active Gammaproteobacterium linking methanotrophy to partial denitrification in an anoxic oxygen minimum zone. Front Mar Sci 4:23. https://doi.org/10.3389/fmars.2017.00023.
105. Egger M, Hagens M, Sapart CJ, Dijkstra N, van Helmond NAGM, Mogollón JM, Risgaard-Petersen N, van der Veen C, Kasten S, Riedinger N, Böttcher ME, Röckmann T, Jørgensen BB, Slomp CP. 2017. Iron oxide reduction in methane-rich deep Baltic Sea sediments. Geochim Cosmochim Acta 207:256–276. https://doi.org/10.1016/j.gca.2017.03.019.
106. Riedinger N, Formolo MJ, Lyons TW, Henkel S, Beck A, Kasten S. 2014. An inorganic geochemical argument for coupled anaerobic oxidation of methane and iron reduction in marine sediments. Geobiology 12:172–181. https://doi.org/10.1111/gbi.12077.
107. Bar-Or I, Elvert M, Eckert W, Kushmaro A, Vigderovich H, Zhu Q, Ben-Dov E, Sivan O. 2017. Iron-coupled anaerobic oxidation of methane performed by a mixed bacterial-archaeal community based on poorly reactive minerals. Environ Sci Technol 51:12293–12301. https://doi.org/10.1021/acs.est.7b03126.
108. Martinez-Cruz K, Leewis MC, Herriott IC, Sepulveda-Jauregui A, Anthony KW, Thalasso F, Leigh MB. 2017. Anaerobic oxidation of methane by aerobic methanotrophs in sub-Arctic lake sediments. Sci Total Environ 607-608: 23–31.
109. Sivan O, Adler M, Pearson A, Gelman F, Bar-Or I, John SG, Eckert W. 2011. Geochemical evidence for iron-mediated anaerobic oxidation of methane. Limnol Oceanogr 56:1536–1544. https://doi.org/10.4319/lo.2011.56.4.1536.
110. Tebo BM. 1991. Manganese(II) oxidation in the suboxic zone of the Black Sea. Deep Sea Res A Oceanogr Res Pap 38:S883–S905. https://doi.org/10.1016/S0198-0149(10)80015-9.
111. Schippers A, Neretin LN, Lavik G, Leipe T, Pollehne F. 2005. Manganese(II) oxidation driven by lateral oxygen intrusions in the western Black Sea. Geochim Cosmochim Acta 69:2241–2252. https://doi.org/10.1016/j.gca.2004.10.016.
112. Kendall M, Boone D. 2006. The order Methanosarcinales, p 244–256. *In* Dworkin M, Falkow S, Rosenberg E, Schleifer K-H, Stackebrandt E (ed), The prokaryotes, volume 3: Archaea. Bacteria: Firmicutes, Actinomycetes. Springer, New York, NY.
113. Lin Y-S, Heuer VB, Goldhammer T, Kellermann MY, Zabel M, Hinrichs K-U. 2012. Towards constraining H_2 concentration in subseafloor sediment: a proposal for combined analysis by two distinct approaches. Geochim Cosmochim Acta 77:186–201. https://doi.org/10.1016/j.gca.2011.11.008.
114. Oremland RS, Polcin S. 1982. Methanogenesis and sulfate reduction: competitive and noncompetitive substrates in estuarine sediments. Appl Environ Microbiol 44:1270–1276.
115. Abram JW, Nedwell DB. 1978. Inhibition of methanogenesis by sulphate reducing bacteria competing for transferred hydrogen. Arch Microbiol 117:89–92. https://doi.org/10.1007/BF00689356.
116. Oremland RS, Marsh LM, Polcin S. 1982. Methane production and simultaneous sulphate reduction in anoxic, salt marsh sediments. Nature 296:143–145. https://doi.org/10.1038/296143a0.
117. McGlynn SE, Chadwick GL, Kempes CP, Orphan VJ. 2015. Single cell activity reveals direct electron transfer in methanotrophic consortia. Nature 526:531–535. https://doi.org/10.1038/nature15512.
118. DeLong EF. 1998. Everything in moderation: Archaea as "non-extremophiles." Curr Opin Genet Dev 8:649–654.
119. Jørgensen BB. 2000. Bacteria and marine biogeochemistry, p 173–207. *In* Schulz HD, Zabel M (ed), Marine geochemistry. Springer, Berlin, Germany.
120. Coolen MJL, Cypionka H, Sass AM, Sass H, Overmann J. 2002. Ongoing modification of Mediterranean Pleistocene sapropels mediated by prokaryotes. Science 296:2407–2410. https://doi.org/10.1126/science.1071893.
121. De Lange GJ, Thomson J, Reitz A, Slomp CP, Speranza Principato M, Erba E, Corselli C. 2008. Synchronous basin-wide formation and redox-controlled preservation of a Mediterranean sapropel. Nat Geosci 1:606–610. https://doi.org/10.1038/ngeo283.
122. Zonneveld KAF, Versteegh GJM, Kasten S, Eglinton TI, Emeis K-C, Huguet C, Koch BP, de Lange GJ, de Leeuw JW, Middelburg JJ, Mollenhauer G, Prahl FG, Rethemeyer J, Wakeham SG. 2010. Selective preservation of organic matter in marine environments; processes and impact on the sedimentary record. Biogeosciences 7:483–511. https://doi.org/10.5194/bg-7-483-2010.
123. Inagaki F, Hinrichs K-U, Kubo Y, Bowles MW, Heuer VB, Hong W-L, Hoshino T, Ijiri A, Imachi H, Ito M, Kaneko M, Lever MA, Lin Y-S, Methe BA, Morita S, Morono Y, Tanikawa W, Bihan M, Bowden SA, Elvert M, Glombitza C, Gross D, Harrington GJ, Hori T, Li K, Limmer D, Liu C-H, Murayama M, Ohkouchi N, Ono S, Park Y-S, Phillips SC, Prieto-Mollar X, Purkey M, Riedinger N, Sanada Y, Sauvage J, Snyder G, Susilawati R, Takano Y, Tasumi E, Terada T, Tomaru H, Trembath-Reichert E, Wang DT, Yamada Y. 2015. Exploring deep microbial life in coal-bearing sediment down to 2.5 km below the ocean floor. Science 349:420–424. https://doi.org/10.1126/science.aaa6882.
124. Orsi WD, Coolen MJL, Wuchter C, He L, More KD, Irigoien X, Chust G, Johnson C, Hemingway JD, Lee M, Galy V, Giosan L. 2017. Climate oscillations reflected within the microbiome of Arabian Sea sediments. Sci Rep 7:6040. https://doi.org/10.1038/s41598-017-05590-9.
125. Ciobanu M-C, Rabineau M, Droz L, Révillon S, Ghiglione J-FJ-F, Dennielou B, Jorry S-JS-J, Kallmeyer J, Etoubleau J, Pignet P, Crassous P, Vandenabeele-Trambouze O, Laugier J, Guégan M, Godfroy A, Alain K. 2012. Sedimentological imprint on subseafloor microbial communities in western Mediterranean Sea quaternary sediments. Biogeosciences 9:3491–3512. https://doi.org/10.5194/bg-9-3491-2012.
126. Inagaki F, Suzuki M, Takai K, Oida H, Sakamoto T, Aoki K, Nealson KH, Horikoshi K. 2003. Microbial communities associated with geological horizons in coastal subseafloor sediments from the Sea of Okhotsk. Appl Environ Microbiol 69:7224–7235. https://doi.org/10.1128/AEM.69.12.7224-7235.2003.
127. Marshall IPG, Karst SM, Nielsen PH, Jørgensen BB. 2018. Metagenomes from deep Baltic Sea sediments reveal how past and present environmental conditions determine microbial community composition. Mar Genomics 37:58–68. https://doi.org/10.1016/j.margen.2017.08.004.
128. Starnawski P, Bataillon T, Ettema TJG, Jochum LM, Schreiber L, Chen X, Lever MA, Polz MF, Jørgensen BB, Schramm A, Kjeldsen KU. 2017. Microbial community assembly and evolution in subseafloor sediment. Proc Natl Acad Sci U S A 114:2940–2945. https://doi.org/10.1073/pnas.1614190114.
129. Schröder JM. 2015. Intact polar lipids in marine sediments: improving

analytical protocols and assessing planktonic and benthic sources. University of Bremen, Bremen, Germany.
130. Biddle JF, Lipp JS, Lever MA, Lloyd KG, Sørensen KB, Anderson R, Fredricks HF, Elvert M, Kelly TJ, Schrag DP, Sogin ML, Brenchley JE, Teske A, House CH, Hinrichs K-U. 2006. Heterotrophic Archaea dominate sedimentary subsurface ecosystems off Peru. Proc Natl Acad Sci U S A 103:3846–3851. https://doi.org/10.1073/pnas.0600035103.
131. Lloyd KG, Schreiber L, Petersen DG, Kjeldsen KU, Lever M a, Steen AD, Stepanauskas R, Richter M, Kleindienst S, Lenk S, Schramm A, Jørgensen BB. 2013. Predominant archaea in marine sediments degrade detrital proteins. Nature 496:215–218. https://doi.org/10.1038/nature12033.
132. Baker BJ, Saw JH, Lind AE, Lazar CS, Hinrichs K, Teske AP, Ettema TJG. 2016. Genomic inference of the metabolism of cosmopolitan subsurface Archaea, Hadesarchaea. Nat Microbiol 1:16002. https://doi.org/10.1038/nmicrobiol.2016.2.
133. Seitz KW, Lazar CS, Hinrichs K-U, Teske AP, Baker BJ. 2016. Genomic reconstruction of a novel, deeply branched sediment archaeal phylum with pathways for acetogenesis and sulfur reduction. ISME J 10:1696–1705. https://doi.org/10.1038/ismej.2015.233.
134. He Y, Li M, Perumal V, Feng X, Fang J, Xie J, Sievert SM, Wang F. 2016. Genomic and enzymatic evidence for acetogenesis among multiple lineages of the archaeal phylum Bathyarchaeota widespread in marine sediments. Nat Microbiol 1:16035. https://doi.org/10.1038/nmicrobiol.2016.35.
135. Lazar CS, Baker BJ, Seitz KW, Teske AP. 2017. Genomic reconstruction of multiple lineages of uncultured benthic archaea suggests distinct biogeochemical roles and ecological niches. ISME J 11:1118–1129. https://doi.org/10.1038/ismej.2016.189.
136. Dodsworth JA, Blainey PC, Murugapiran SK, Swingley WD, Ross CA, Tringe SG, Chain PSG, Scholz MB, Lo C-C, Raymond J, Quake SR, Hedlund BP. 2013. Single-cell and metagenomic analyses indicate a fermentative and saccharolytic lifestyle for members of the OP9 lineage. Nat Commun 4:1854. https://doi.org/10.1038/ncomms2884.
137. Nobu MK, Dodsworth JA, Murugapiran SK, Rinke C, Gies EA, Webster G, Schwientek P, Kille P, Parkes RJ, Sass H, Jørgensen BB, Weightman AJ, Liu W-T, Hallam SJ, Tsiamis G, Woyke T, Hedlund BP. 2016. Phylogeny and physiology of candidate phylum "Atribacteria" (OP9/JS1) inferred from cultivation-independent genomics. ISME J 10:273–286. https://doi.org/10.1038/ismej.2015.97.
138. Das A, Hugenholtz J, Van Halbeek H, Ljungdahl LG. 1989. Structure and function of a menaquinone involved in electron transport in membranes of *Clostridium thermoautotrophicum* and *Clostridium thermoaceticum*. J Bacteriol 171:5823–5829. https://doi.org/10.1128/jb.171.11.5823-5829.1989.
139. Gottwald M, Andreesen JR, LeGall J, Ljungdahl LG. 1975. Presence of cytochrome and menaquinone in *Clostridium formicoaceticum* and *Clostridium thermoaceticum*. J Bacteriol 122:325–328.
140. Hale MB, Blankenship RE, Fuller RC. 1983. Menaquinone is the sole quinone in the facultatively aerobic green photosynthetic bacterium *Chloroflexus aurantiacus*. Biochim Biophys Acta 723:376–382. https://doi.org/10.1016/0005-2728(83)90044-0.
141. Blazejak A, Schippers A. 2010. High abundance of JS-1- and *Chloroflexi*-related *Bacteria* in deeply buried marine sediments revealed by quantitative, real-time PCR. FEMS Microbiol Ecol 72:198–207. https://doi.org/10.1111/j.1574-6941.2010.00838.x.
142. Thauer RK, Kaster A-K, Seedorf H, Buckel W, Hedderich R. 2008. Methanogenic archaea: ecologically relevant differences in energy conservation. Nat Rev Microbiol 6:579–591. https://doi.org/10.1038/nrmicro1931.
143. Becker KW, Elling FJ, Yoshinaga MY, Söllinger A, Urich T, Hinrichs K-U. 2016. Unusual butane- and pentanetriol-based tetraether lipids in *Methanomassiliicoccus luminyensis*, a representative of the seventh order of methanogens. Appl Environ Microbiol 82:4505–4516. https://doi.org/10.1128/AEM.00772-16.
144. Evans PN, Parks DH, Chadwick GL, Robbins SJ, Orphan VJ, Golding SD, Tyson GW. 2015. Methane metabolism in the archaeal phylum Bathyarchaeota revealed by genome-centric metagenomics. Science 350:434–438. https://doi.org/10.1126/science.aac7745.
145. Zabel M, Aiello I, Becker K, Braum S, Broda N, Dibke C, Elvert M, Gagen E, Goldhammer T, Heuer V, Hinrichs K-U, Koch BP, Lazar C, Lin Y-S, Lipp J, Meador T, Pape S, Peters C, Schmal J, Schmidt F, Schröder J, Teske A, Wendt J, Wörmer L, Yoshinaga M, Zhu C, Knuth E, Gogou A, Schön A. 2011. Biogeochemistry and methane hydrates of the Black Sea; oceanography of the Mediterranean; shelf sedimentation and cold water carbonates. RV *Meteor* cruise report M84/L1, DFG Senatskommission für Ozeanographie, Bonn, Germany.
146. Xie S, Liu X-L, Schubotz F, Wakeham SG, Hinrichs K-U. 2014. Distribution of glycerol ether lipids in the oxygen minimum zone of the eastern tropical North Pacific Ocean. Org Geochem 71:60–71. https://doi.org/10.1016/j.orggeochem.2014.04.006.
147. Stookey LL. 1970. Ferrozine—a new spectrophotometric reagent for iron. Anal Chem 42:779–781. https://doi.org/10.1021/ac60289a016.
148. Hall POJ, Aller RC. 1992. Rapid, small-volume, flow injection analysis for CO_2 and NH_4^+ in marine and freshwaters. Limnol Oceanogr 37:1113–1119. https://doi.org/10.4319/lo.1992.37.5.1113.
149. Cline JD. 1969. Spectrophotometric determination of hydrogen sulfide in natural waters. Limnol Oceanogr 14:454–458. https://doi.org/10.4319/lo.1969.14.3.0454.
150. Kvenvolden KA, McDonald TJ. 1986. Organic geochemistry on JOIDES resolution—an essay. Texas A&M University, College Station, TX.
151. D'Hondt SL, Jørgensen BB, Miller DJ. 2003. Proceedings of the ocean drilling program, initial reports, 201. Texas A&M University, College Station, TX.
152. Ertefai TF, Heuer VB, Prieto Mollar X, Vogt C, Sylva SP, Seewald J, Hinrichs K-U. 2010. The biogeochemistry of sorbed methane in marine sediments. Geochim Cosmochim Acta 74:6033–6048. https://doi.org/10.1016/j.gca.2010.08.006.
153. Schmidt F, Koch BP, Goldhammer T, Elvert M, Witt M, Lin YS, Wendt J, Zabel M, Heuer VB, Hinrichs KU. 2017. Unraveling signatures of biogeochemical processes and the depositional setting in the molecular composition of pore water DOM across different marine environments. Geochim Cosmochim Acta 207:57–80. https://doi.org/10.1016/j.gca.2017.03.005.
154. Zhu C, Lipp JS, Wörmer L, Becker KW, Schröder J, Hinrichs K-U. 2013. Comprehensive glycerol ether lipid fingerprints through a novel reversed phase liquid chromatography-mass spectrometry protocol. Org Geochem 65:53–62. https://doi.org/10.1016/j.orggeochem.2013.09.012.
155. Becker KW, Lipp JS, Zhu C, Liu X-L, Hinrichs K-U. 2013. An improved method for the analysis of archaeal and bacterial ether core lipids. Org Geochem 61:34–44. https://doi.org/10.1016/j.orggeochem.2013.05.007.
156. Rechka JA, Maxwell JR. 1988. Characterisation of alkenone temperature indicators in sediments and organisms. Org Geochem 13:727–734. https://doi.org/10.1016/0146-6380(88)90094-0.
157. R Core Team. 2013. R: a language and environment for statistical computing. http://www.r-project.org/. R Foundation, Vienna, Austria.
158. Oksanen J, Blanchet FG, Friendly M, Kindt R, Legendre P, McGlinn D, Minchin PR, O'Hara RB, Simpson GL, Solymos P, Stevens MHH, Szoecs E, Wagner H. 2017. vegan: community ecology package. https://cran.r-project.org/package=vegan.
159. Wessel P, Smith WHF, Scharroo R, Luis J, Wobbe F. 2013. Generic Mapping Tools: improved version released. EOS (Washington, DC) 95:409–410.
160. Rosenberg E, DeLong EF, Lory S, Stackebrandt E, Thompson F. 2006. The prokaryotes—actinobacteria, 4th ed. Springer, Berlin, Germany.